Physics Potentials with the Second Hyper-Kamiokande Detector in Korea

(Hyper-Kamiokande Proto-Collaboration)

K. Abe,[57, 59] Ke. Abe,[24] H. Aihara,[59, 60] A. Aimi,[18] R. Akutsu,[58] C. Andreopoulos,[28, 43]
I. Anghel,[21] L.H.V. Anthony,[28] M. Antonova,[20] Y. Ashida,[25] M. Barbi,[44] G.J. Barker,[66]
G. Barr,[40] P. Beltrame,[11] V. Berardi,[16] M. Bergevin,[3] S. Berkman,[2] T. Berry,[45]
S. Bhadra,[73] F.d.M. Blaszczyk,[1] A. Blondel,[12] S. Bolognesi,[6] S.B. Boyd,[66] A. Bravar,[12]
C. Bronner,[59] M. Buizza Avanzini,[10] F.S. Cafagna,[16] A. Cole,[50] R. Calland,[59] S. Cao,[25]
S.L. Cartwright,[50] M.G. Catanesi,[16] C. Checchia,[18] Z. Chen-Wishart,[45] J.H. Choi,[8]
K. Choi,[14] J. Coleman,[28] G. Collazuol,[18] G. Cowan,[11] L. Cremonesi,[48] T. Dealtry,[27]
G. De Rosa,[17] C. Densham,[43] D. Dewhurst,[40] E.L. Drakopoulou,[11] F. Di Lodovico,[48]
O. Drapier,[10] P. Dunne,[15] M. Dziewiecki,[65] S. Emery,[6] A. Esmaili,[46] P. Fernández,[31]
E. Fernández-Martinez,[31] T. Feusels,[2] A. Finch,[27] A. Fiorentini,[73] M. Fitton,[43]
K. Frankiewicz,[37] M. Friend,[22] Y. Fujii,[22] Y. Fukuda,[33] D. Fukuda,[38] K. Ganezer,[5]
M. Gonin,[10] N. Grant,[66] P. Gumplinger,[62] D.R. Hadley,[66] L. Haegel,[12] D. Hamabe,[61]
B. Hartfiel,[5] M. Hartz,[59, 62] Y. Hayato,[57, 59] K. Hayrapetyan,[48] J. Hill,[5] S. Hirota,[25]
S. Horiuchi,[69] A.K. Ichikawa,[25] T. Iijima,[34, 35] M. Ikeda,[57] J. Imber,[10] K. Inoue,[55, 59]
J. Insler,[30] R.A. Intonti,[16] A. Ioannisian,[72] T. Ishida,[22] H. Ishino,[38] M. Ishitsuka,[61]
Y. Itow,[35, 36] K. Iwamoto,[47] A. Izmaylov,[20] B. Jamieson,[68] H.I. Jang,[52] J.S. Jang,[13]
S.H. Jeon,[54] M. Jiang,[25] P. Jonsson,[15] K.K. Joo,[7] A. Kaboth,[43, 45] C. Kachulis,[1]
T. Kajita,[58, 59] J. Kameda,[57, 59] Y. Karadhzov,[12] T. Katori,[48] K. Kayrapetyan,[48]
E. Kearns,[1, 59] M. Khabibullin,[20] A. Khotjantsev,[20] J.H. Kim,[54] J.Y. Kim,[7] S.B. Kim,[51]
S.Y. Kim,[51] S. King,[48] Y. Kishimoto,[57, 59] P. Ko*,[23] T. Kobayashi,[22] M. Koga,[55, 59]
A. Konaka,[62] L.L. Kormos,[27] Y. Koshio,[38, 59] K.L. Kowalik,[37] W.R. Kropp,[4] Y. Kudenko,[20]
R. Kurjata,[65] T. Kutter,[30] M. Kuze,[61] L. Labarga,[31] J. Lagoda,[37] P.J.J. Lasorak,[48]
M. Laveder,[18] M. Lawe,[27] J.G. Learned,[14] I.T. Lim,[7] T. Lindner,[62] R. P. Litchfield,[15]
A. Longhin,[18] P. Loverre,[19] T. Lou,[60] L. Ludovici,[19] W. Ma,[15] L. Magaletti,[16] K. Mahn,[32]
M. Malek,[50] L. Maret,[12] C. Mariani,[69] K. Martens,[59] Ll. Marti,[57] J.F. Martin,[63] J. Marzec,[65]

1

S. Matsuno,[14] E. Mazzucato,[6] M. McCarthy,[73] N. McCauley,[28] K.S. McFarland,[47]

C. McGrew,[53] A. Mefodiev,[20] C. Metelko,[28] M. Mezzetto,[18] J. Migenda,[50] P. Mijakowski,[37]

H. Minakata,[71] A. Minamino,[25] S. Mine,[4] O. Mineev,[20] M. Miura,[57,59] J. Monroe,[45]

D.H. Moon,[7] S. Moriyama,[57,59] T. Mueller,[10] F. Muheim,[11] K. Murase,[41] F. Muto,[34]

M. Nakahata,[57,59] Y. Nakajima,[57] K. Nakamura,[22,59] T. Nakaya,[25,59] S. Nakayama,[57,59]

C. Nantais,[63] M. Needham,[11] T. Nicholls,[43] Y. Nishimura,[58] E. Noah,[12] F. Nova,[43]

J. Nowak,[27] H. Nunokawa,[46] Y. Obayashi,[59] H.M. O'Keeffe,[27] Y. Okajima,[61]

K. Okumura,[58,59] E. O'Sullivan,[9] T. Ovsiannikova,[20] R.A. Owen,[48] Y. Oyama,[22] J. Pérez,[31]

M.Y. Pac,[8] V. Palladino,[17] J.L. Palomino,[53] V. Paolone,[42] W. Parker,[45] S. Parsa,[12]

D. Payne,[28] J.D. Perkin,[50] E. Pinzon Guerra,[73] S. Playfer,[11] M. Posiadala-Zezula,[64]

J.-M. Poutissou,[62] A. Pritchard,[28] N.W. Prouse,[48] P. Przewlocki,[37] B. Quilain,[25]

M. Quinto,[16] E. Radicioni,[16] P.N. Ratoff,[27] M.A. Rayner,[12] F. Retiere,[62] C. Riccio,[17]

B. Richards,[48] E. Rondio,[37] H.J. Rose,[28] C. Rott,[54] S.D. Rountree,[69] A.C. Ruggeri,[17]

A. Rychter,[65] R. Sacco,[48] M. Sakuda,[38] M.C. Sanchez,[21] E. Scantamburlo,[12]

K. Scholberg,[9,59] M. Scott,[62] Y. Seiya,[39] T. Sekiguchi,[22] H. Sekiya,[57,59] S.H. Seo,[51]

D. Sgalaberna,[12] R. Shah,[40] A. Shaikhiev,[20] I. Shimizu,[55] M. Shiozawa,[57,59] Y. Shitov,[15,45]

S. Short,[48] C. Simpson,[40,59] G. Sinnis,[29] M.B. Smy,[4,59] S. Snow,[66] J. Sobczyk,[70]

H.W. Sobel,[4,59] Y. Sonoda,[57] T. Stewart,[43] J.L. Stone,[1,59] Y. Suda,[60] Y. Suwa,[74]

Y. Suzuki,[59] A.T. Suzuki,[24] R. Svoboda,[3] R. Tacik,[44] A. Takeda,[57] A. Takenaka,[57]

A. Taketa,[56] Y. Takeuchi,[24,59] V. Takhistov,[4] H.A. Tanaka,[63] H.K.M. Tanaka,[56]

H. Tanaka,[57,59] R. Terri,[48] L.F. Thompson,[50] M. Thorpe,[43] S. Tobayama,[2] T. Tomura,[57,59]

C. Touramanis,[28] T. Towstego,[63] T. Tsukamoto,[22] K.M. Tsui,[58] M. Tzanov,[30]

Y. Uchida,[15] M.R. Vagins,[4,59] G. Vasseur,[6] C. Vilela,[53] R.B. Vogelaar,[69] J. Walding,[45]

C.W. Walter,[9,59] D. Wark,[40,43] M.O. Wascko,[15] A. Weber,[43] R. Wendell,[25,59] R.J. Wilkes,[67]

M.J. Wilking,[53] J.R. Wilson,[48] T. Xin,[21] K. Yamamoto,[39] C. Yanagisawa,[53] T. Yano,[24]

S. Yen,[62] N. Yershov,[20] D.N. Yeum,[51] M. Yokoyama,[59,60] T. Yoshida,[61] I. Yu,[54]

M. Yu,[73] J. Zalipska,[37] K. Zaremba,[65] M. Ziembicki,[65] M. Zito,[6] and S. Zsoldos[48]

(Hyper-Kamiokande proto-collaboration)

[1]*Boston University, Department of Physics, Boston, Massachusetts, U.S.A.*

[2]*University of British Columbia, Department of Physics*

2

and Astronomy, Vancouver, British Columbia, Canada

[3] *University of California, Davis, Department of Physics, Davis, California, U.S.A.*

[4] *University of California, Irvine, Department of*

Physics and Astronomy, Irvine, California, U.S.A.

[5] *California State University, Department of Physics, Carson, California, U.S.A.*

[6] *IRFU, CEA Saclay, Gif-sur-Yvette, France*

[7] *Chonnam National University, Department of Physics, Gwangju, Korea*

[8] *Dongshin University, Basic Science Research Institute, Naju, Korea*

[9] *Duke University, Department of Physics, Durham, North Carolina, U.S.A.*

[10] *Ecole Polytechnique, IN2P3-CNRS, Laboratoire Leprince-Ringuet, Palaiseau, France*

[11] *University of Edinburgh, School of Physics and Astronomy, Edinburgh, United Kingdom*

[12] *University of Geneva, Section de Physique, DPNC, Geneva, Switzerland*

[13] *GIST College, Gwangju Institute of Science and Technology, Gwangju 500-712, Korea*

[14] *University of Hawaii, Department of Physics and Astronomy, Honolulu, Hawaii, U.S.A.*

[15] *Imperial College London, Department of Physics, London, United Kingdom*

[16] *INFN Sezione di Bari and Università e Politecnico di*

Bari, Dipartimento Interuniversitario di Fisica, Bari, Italy

[17] *INFN Sezione di Napoli and Università di Napoli, Dipartimento di Fisica, Napoli, Italy*

[18] *INFN Sezione di Padova and Università di Padova, Dipartimento di Fisica, Padova, Italy*

[19] *INFN Sezione di Roma, Roma, Italy*

[20] *Institute for Nuclear Research of the Russian Academy of Sciences, Moscow, Russia*

[21] *Iowa State University, Department of Physics and Astronomy, Ames, Iowa, U.S.A.*

[22] *High Energy Accelerator Research Organization (KEK), Tsukuba, Ibaraki, Japan*

[23] *Korean Institute for Advanced Studies, Seoul, Korea*

[24] *Kobe University, Department of Physics, Kobe, Japan*

[25] *Kyoto University, Department of Physics, Kyoto, Japan*

[26] *Laboratori Nazionali di Frascati, Frascati, Italy*

[27] *Lancaster University, Physics Department, Lancaster, United Kingdom*

[28] *University of Liverpool, Department of Physics, Liverpool, United Kingdom*

[29] *Los Alamos National Laboratory, New Mexico, U.S.A.*

[30] *Louisiana State University, Department of Physics*

and Astronomy, Baton Rouge, Louisiana, U.S.A.

[31]University Autonoma Madrid, Department of Theoretical Physics, Madrid, Spain

[32]Michigan State University, Department of Physics
and Astronomy, East Lansing, Michigan, U.S.A.

[33]Miyagi University of Education, Department of Physics, Sendai, Japan

[34]Nagoya University, Graduate School of Science, Nagoya, Japan

[35]Nagoya University, Kobayashi-Maskawa Institute for
the Origin of Particles and the Universe, Nagoya, Japan

[36]Nagoya University, Institute for Space-Earth Environmental Research, Nagoya, Japan

[37]National Centre for Nuclear Research, Warsaw, Poland

[38]Okayama University, Department of Physics, Okayama, Japan

[39]Osaka City University, Department of Physics, Osaka, Japan

[40]Oxford University, Department of Physics, Oxford, United Kingdom

[41]Pennsylvania State University, Department of Physics, University Park, PA 16802, U.S.A.

[42]University of Pittsburgh, Department of Physics
and Astronomy, Pittsburgh, Pennsylvania, U.S.A.

[43]STFC, Rutherford Appleton Laboratory, Harwell Oxford,
and Daresbury Laboratory, Warrington, United Kingdom

[44]University of Regina, Department of Physics, Regina, Saskatchewan, Canada

[45]Royal Holloway University of London, Department
of Physics, Egham, Surrey, United Kingdom

[46]Pontifícia Universidade Católica do Rio de Janeiro,
Departamento de Física, Rio de Janeiro, Brazil

[47]University of Rochester, Department of Physics
and Astronomy, Rochester, New York, U.S.A.

[48]Queen Mary University of London, School of
Physics and Astronomy, London, United Kingdom

[49]Universidade de São Paulo, Instituto de Física, São Paulo, Brazil

[50]University of Sheffield, Department of Physics and Astronomy, Sheffield, United Kingdom

[51]Seoul National University, Department of Physics, Seoul, Korea

[52]Seoyeong University, Department of Fire Safety, Gwangju, Korea

[53]State University of New York at Stony Brook, Department
of Physics and Astronomy, Stony Brook, New York, U.S.A.

[54]Sungkyunkwan University, Department of Physics, Suwon, Korea

[55]Research Center for Neutrino Science, Tohoku University, Sendai, Japan

[56]University of Tokyo, Earthquake Research Institute, Tokyo, Japan

[57]University of Tokyo, Institute for Cosmic Ray
Research, Kamioka Observatory, Kamioka, Japan

[58]University of Tokyo, Institute for Cosmic Ray Research,
Research Center for Cosmic Neutrinos, Kashiwa, Japan

[59]University of Tokyo, Kavli Institute for the Physics and Mathematics of the
Universe (WPI), Todai Institutes for Advanced Study, Kashiwa, Chiba, Japan

[60]University of Tokyo, Department of Physics, Tokyo, Japan

[61]Tokyo Institute of Technology, Department of Physics, Tokyo, Japan

[62]TRIUMF, Vancouver, British Columbia, Canada

[63]University of Toronto, Department of Physics, Toronto, Ontario, Canada

[64]University of Warsaw, Faculty of Physics, Warsaw, Poland

[65]Warsaw University of Technology, Institute of
Radioelectronics and Multimedia Technology, Warsaw, Poland

[66]University of Warwick, Department of Physics, Coventry, United Kingdom

[67]University of Washington, Department of Physics, Seattle, Washington, U.S.A.

[68]University of Winnipeg, Department of Physics, Winnipeg, Manitoba, Canada

[69]Virginia Tech, Center for Neutrino Physics, Blacksburg, Virginia, U.S.A.

[70]Wroclaw University, Faculty of Physics and Astronomy, Wroclaw, Poland

[71]Yachay Tech, Department of Physics, San Miguel de Urcuquí, Ecuador

[72]Yerevan Institute for Theoretical Physics and
Modeling, Halabian Str. 34; Yerevan 0036, Armenia

[73]York University, Department of Physics and Astronomy, Toronto, Ontario, Canada

[74]Kyoto University, Yukawa Institute for Theoretical Physics, Kyoto, Japan

Abstract

We have conducted sensitivity studies on an alternative configuration of the Hyper-Kamiokande experiment by locating the 2nd Hyper-Kamiokande detector in Korea at $\sim 1100-1300$ km baseline. Having two detectors at different baselines improves sensitivity to leptonic CP violation, neutrino mass ordering as well as nonstandard neutrino interactions. There are several candidate sites in Korea with greater than 1 km high mountains ranged at an $1-3$ degree off-axis angle. Thanks to larger overburden of the candidate sites in Korea, low energy physics, such as solar and supernova neutrino physics as well as dark matter search, is expected to be improved. In this paper sensitivity studies on the CP violation phase and neutrino mass ordering are performed using current T2K systematic uncertainties in most cases. We plan to improve our sensitivity studies in the near future with better estimation of our systematic uncertainties.

I. MOTIVATION

The Hyper-Kamiokande (Hyper-K or HK) proposal [1] builds upon the highly successful Super-Kamiokande (Super-K or SK) detector [2] by constructing water Cherenkov detectors with nearly twenty times the fiducial volume of SK to pursue a rich program of neutrino (astro)physics and proton decay. The current Hyper-K design calls for the staged construction of two 187 kt (fiducial volume mass) modules near the current Super-K site, 295 km away and 2.5° off-axis (OA) from the J-PARC neutrino beam used by the T2K experiment. The long baseline neutrino program at Hyper-K with the J-PARC neutrino beam aims for a definitive observation of CP violation (CPV) in neutrino oscillations that may result from an irreducible phase δ_{CP} in the neutrino mixing matrix. Hyper-K will make precise measurements of other oscillation parameters, such as the mixing angle θ_{23} and Δm_{32}^2, and thus will provide highly sensitive tests of the three-flavor mixing paradigm. These measurements are valuable towards elucidating the new physics responsible for neutrino mass and mixing and its potential connections to the mystery of the matter/antimatter asymmetry of the universe.

In this document, we will explore the possibility of placing one of the two Hyper-K modules in Korea at a baseline of $1000-1300$ km; we will refer to this as "T2HKK" in contrast to the current default configuration with both detectors in Kamioka with 295 km baseline ("T2HK") . The T2HKK configuration, which provides measurements at two significantly different baselines, will break degeneracies related to the unknown mass ordering, θ_{23}, and the CP-violating phase δ_{CP}. It will provide the opportunity to fully probe the oscillation physics at the first and second oscillation maxima. The measurements at multiple baselines, including near detectors at J-PARC, can serve to mutually reduce systematic uncertainties across all the measurements. The study of non-standard neutrino interactions is also expected to be significantly enhanced by the two-baseline configuration.

In Korea, the range of OA angle from J-PARC is 1 to 3 degree (see Fig. 1), and within this range there are many mountains over 1 km height. This allows for the optimization of the OA angle within this range based on physics sensitivities and systematic error considerations. It also provides an enhanced program of low energy physics such as solar neutrino, supernova and dark matter neutrino detection studies, and geophysics that would benefit from the large overburden in the Korean site. Recent developments in gadolinium doping of water and
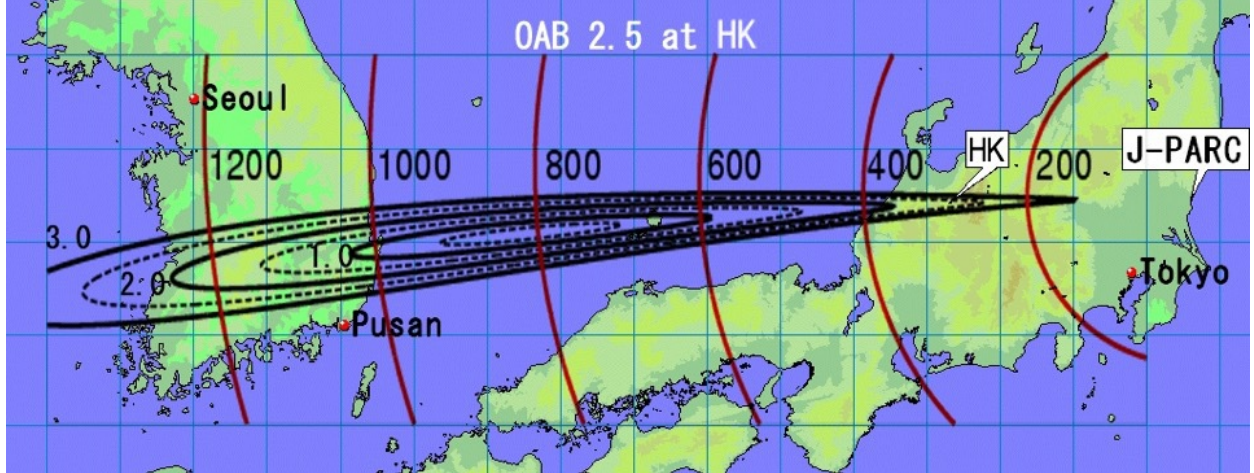
FIG. 1: Contour map of the J-PARC off-axis beam to Korea [8, 9].

water-based liquid scintillators raise the possibility of a program based on reactor neutrinos at a later stage.

There were earlier efforts on a large water Cherenkov detector in Korea using a J-PARC-based neutrino beam [3, 4]. Originally an idea for a two baseline experiment with a 2nd detector in Korea has been discussed by several authors pointing out possible improvements for measurements on CP violation and mass hierarchy [5–9]. Three international workshops were held in Korea and Japan in 2005, 2006 and 2007 [10]. The mixing angle of θ_{13} was not known yet, and therefore the detector size and mass could not be determined at the time. Now more realistic studies and a detector design are possible due to the precisely measured θ_{13} [11–18].

Overall the T2HKK configuration with two baselines offers the possibility to significantly augment the study of neutrino oscillations relative to the single baseline T2HK configuration. The resolution of parameter degeneracies with the measurement at two baselines also may allow for more precise measurements of the oscillation parameters and sensitivity to non-standard physics. In the following sections more details on the T2HKK detector, sensitivity studies, and additional benefits are discussed followed by a summary and conclusion.

II. SECOND HYPER-KAMIOKANDE DETECTOR IN KOREA

In this chapter we present an experimental setup and physics sensitivities of the second Hyper-K detector in Korea using the J-PARC neutrino beam.

A. J-PARC neutrino beam and Hyper-K detector

The J-PARC neutrino beam and the Hyper-K detector with the near and intermediate detectors will be described in the next subsections.

1. J-PARC neutrino beam

The neutrino beam for Hyper-K is produced at J-PARC (Japan Proton Accelerator Research Complex) located in Tokai Village, Ibaraki prefecture, on the east coast of Japan, 295 km from the Kamioka detector sites. The 30-GeV (kinetic energy) proton beam is extracted from the J-PARC Main Ring (MR) by single-turn fast extraction and transported to the production target after being deflected about 90° by 28 superconducting combined function magnets to direct the beam towards Kamioka. The beam pulse consists of 8 bunches spaced 581 ns apart to give a 4.2 μs total pulse length. The repetition period of the pulse is 2.48 s as of 2016. The production target is a 26 mm diameter and 90 cm long graphite rod (corresponding to 2 interaction lengths). About 80% of incoming protons interact in the target. The secondary pions (and kaons) from the target are focused by three consecutive electromagnetic horns operated by a 250 kA pulsed current. The focused pions and kaons enter a 110 m length decay volume (DV) filled with helium gas and decay in flight into neutrinos. The beam dump, which consists of graphite blocks of about 3.15 m thickness followed by iron plates of 2.5 m total thickness, is placed at the end of the DV to absorb remnant hadrons. Muon monitors (MUMONs) are placed just behind the beam dump to monitor on a spill-by-spill basis the intensity and the profile of muons > 5 GeV which pass through the beam dump.

The J-PARC neutrino beamline adopted the first ever off-axis scheme to produce a narrow energy neutrino spectrum centered at oscillation maximum to maximize the physics sensitivity. The T2K experiment is now running at a 2.5 degree off-axis angle to the Super-Kamiokande detector. The J-PARC neutrino beamline is designed to accommodate $2 \sim 2.5°$

off-axis angle at the current Super-Kamiokande and proposed Hyper-Kamiokande sites.

As of summer 2016, stable operation of the MR at 425 kW beam power has been achieved. In 2018, the design power of 750 kW will be realized by increasing the repetition rate from 1/2.48 s to 1/1.3 s by upgrading magnet power supplies, RF core and other components. Further beam power increases will require upgrades to secondary beamline components such as the beam window, target, and horns. Upgrades primarily to the RF power supply will gradually increase the number of protons/pulse (ppp) and repetition rate further to 330 Tp and 1/1.16 s, respectively, to reach > 1.3 MW by around 2025 before Hyper-K becomes operational.

2. Hyper-Kamiokande tank configuration

The Hyper-K experiment employs a ring-imaging water Cherenkov detector technique to detect rare interactions of neutrinos and the possible spontaneous decay of protons and bound neutrons. The baseline detector configuration consists of two cylindrical tanks with the second tank commencing operation later than the first tank. The first priority is to perform a CP violation measurement at the earliest opportunity with the first tank.

A full overview of the cavern and detector design R&D, upgraded beam and near detector suite, and expected physics sensitivities can be found in the Hyper-Kamiokande Design Report [19]. The schematic view of each tank is shown in Fig. 2. It is a standing cylindrical tank with a diameter of 74 m and height of 60 m. The total (fiducial) mass of the detector is 258 (187) kilo-tons. Two tanks in total will provide the fiducial volume which is about 20 times larger than that of Super-K. The Hyper-K detector candidate site, located 8 km south of Super-K and 295 km away from J-PARC, is in the Tochibora mine which is used by the Kamioka Mining and Smelting Company near Kamioka town in Gifu Prefecture, Japan. The J-PARC neutrino beamline is designed so that the existing Super-Kamiokande detector in the Mozumi mine and the Hyper-K candidate site in the Tochibora mine have the same off-axis angle. The detector will lie under the peak of Nijuugo-yama, with an overburden of 650 meters of rock or 1,750 meters-water-equivalent (m.w.e.), at geographic coordinates Lat. 36°21'20.105"N, Long.137°18'49.137"E (world geographical coordinate system), and an altitude of 514 m above sea level (a.s.l.).

The Hyper-K detector is designed to employ newly developed high-efficiency and high-
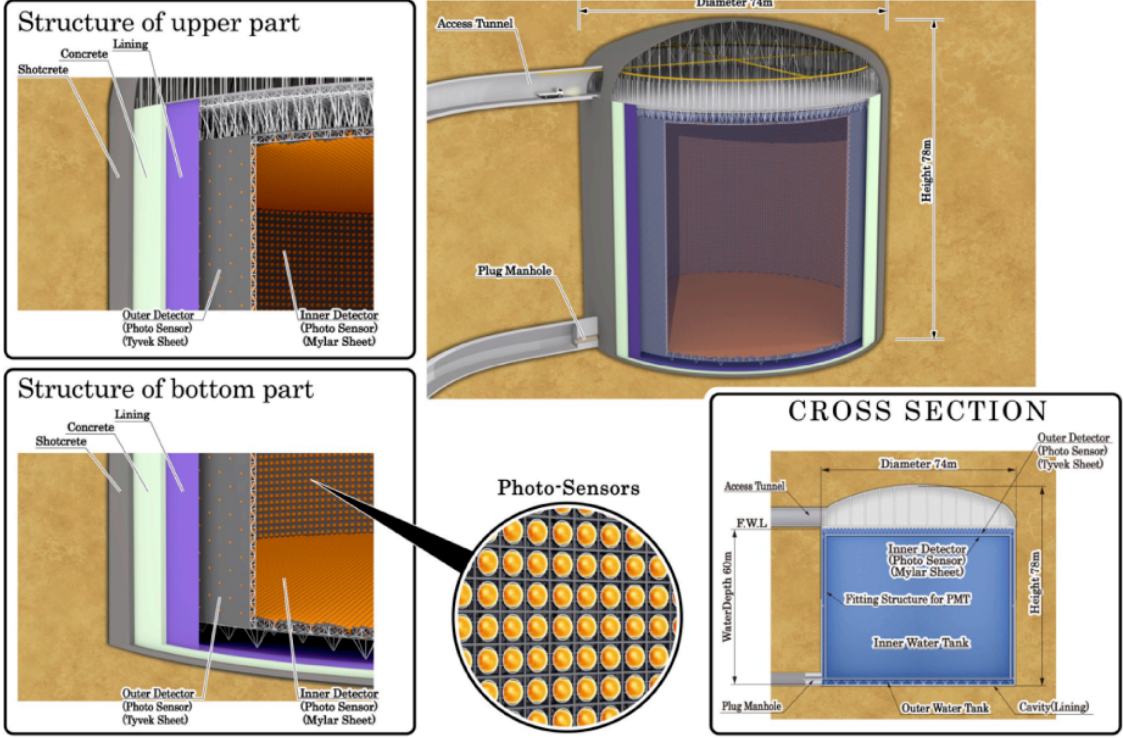
FIG. 2: Schematic view for the first tank.

resolution PMTs (Hamamatsu R12860) which will amplify faint signatures such as those of neutrons associated with neutrino interactions, nuclear de-excitation gammas and π^+ in proton decays into kaons, and so on. This increased sensitivity contributes significantly to the major goals of the Hyper-K experiment such as clean proton decay searches via $p \rightarrow e^+ + \pi^0$ and $p \rightarrow \bar{\nu} + K^+$ decay modes and the observation of supernova electron anti-neutrinos. The inner detector region of the single tank is viewed by 40,000 PMTs, corresponding to the PMT density of 40% photo-cathode coverage (same as that of Super-K). The detector is instrumented with front-end electronics and a readout network/computer system. The system is capable of high-efficiency data acquisition for two successive events in which Michel electron events follow muon events with a mean interval of $2\,\mu\text{sec}$. It is also able to collect the vast amount of neutrinos, which come from a nearby supernova in a nominal time period of $10\,\text{sec}$. Similar to Super-K, an outer detector (OD) with the layer width of $1-2\,\text{m}$ is envisaged that, in addition to enabling additional physics, would help to constrain the external background. Sparser photo-coverage using smaller PMTs than those used for the ID is also planned.

3. Near and intermediate detector complex

The neutrino flux and cross-section models can be constrained by data collected at near detectors, situated close enough to the neutrino production point so that oscillation effects are negligible. Their data addresses important uncertainties in the neutrino flux or cross-section modeling.

The T2K ND280 detector suite comprises two detectors [20]: INGRID, which consists of 16 iron-scintillator modules in a cross pattern centered on the neutrino beam axis, and ND280, a multi-component detector at an angle of 2.5 degree from the beam direction. The primary purpose of the INGRID detector is to constrain the neutrino beam direction, whilst the off-axis detector is used to characterize the neutrino beam before oscillation. T2K has successfully applied a method of fitting to ND280 data with parameterized models of the neutrino flux and interaction cross-sections. Using the ND280 measurements, the systematic uncertainties on the parts of the models constrained by ND280 have been reduced to 3% on the Super-K (SK) predicted event rates. An upgrade of the current ND280 detector is planned before the starting of Hyper-K.

Moreover, a water Cherenkov detector at about 1-2 km is proposed to be built possibly before Hyper-K becomes operational [21]. A water Cherenkov near detector can be used to measure the cross section on H_2O directly, with the same solid angle acceptance as the far detector with no need for a subtraction analysis. Additionally, water Cherenkov detectors have shown excellent particle identification capabilities, allowing for the detection of pure ν_μ-CC, ν_e-CC and NCπ^0 samples. The CCπ^0 rate and kaon production in neutrino interactions, which are backgrounds to nucleon decay searches, can also be measured.

These additional water Cherenkov measurements are essential to achieve the low systematic errors required by Hyper-K, but are complemented by the ND280 magnetized tracking detector, which has the capabilities to track particles below the threshold to produce Cherenkov light in water and to separate neutrino and antineutrino charged current interactions via the lepton charge measurement. Hence a combination of a magnetized tracking detector such as ND280 and the water Cherenkov detector should have the largest impact to reduce systematic uncertainties.

B.   T2HKK Experimental Setup and HKK Candidate Site

The axis of the J-PARC neutrino beam emerges upwards out of the sea between Japan and Korea. The southern part of the Korean peninsula is exposed to the $1-3$ degree off-axis neutrino beams with baselines of $1000-1300$ km as shown in Fig. 1. As mentioned earlier, the T2HKK experiment consists of the first Hyper-K detector in Kamioka at 295 km baseline and the second one in Korea at $\sim$1100 km. In this document, we assume that HKK will be a 258 kt water Cherenkov detector identical to the Hyper-K in Kamioka.

The second oscillation maximum takes place near $E_\nu = 0.6$ GeV at the $\sim$1100 km baseline. The clear separation of different CP phases and mass orderings is observed at the second oscillation maximum. The HKK can be the most sensitive to the CP phase determination if it is placed at 2.5 degrees of off-axis angle, the same as Hyper-K in Kamioka. In that case, the J-PARC neutrino beam spectrum peaks at $E_\nu = 0.6$ GeV with a narrow energy band as shown in Fig. 3. Having identical off-axis angles of the J-PARC beam for HK and HKK, a ratio measurement between HK and HKK would greatly reduce the uncertainties of the neutrino beam flux and spectrum. On the other hand, the maximum sensitivity for determining the neutrino mass ordering is possible by a neutrino beam of $E_\nu > 1$ GeV where the first oscillation maximum takes place. The J-PARC neutrino beam spectrum peaks above 1 GeV with a wider energy band when its off-axis angle is less than 1.5 degrees. In this case, the neutrino flux becomes less in the energy region of the second-oscillation maximum, but still remains enough for the satisfactory CP-phase sensitivity.

The Korean rocks are in general made of granite, hard enough to build a large cavern. A search for mountains higher than 1000 m has been made to find several candidates for HKK as listed in Table I. Mountains in the national or provincial parks are not considered in the search. Two candidate sites are selected among those as shown in Fig. 4: Mt. Bisul at 1.3 degrees of off-axis angle and Mt. Bohyun at 2.2 degrees.

The Mt. Bisul is located at Dalseong in the city of Daegu, the third largest city in South Korea as shown in Fig. 4. Its accessibility is excellent. It takes one and half hours to get to Daegu from Seoul by a Korean bullet train, called KTX. The mountain is 1084 m high and made of hard rocks, granite porphyry and andesitic breccia. HKK is expected to have at least $\sim$820 m overburden and to be exposed to a 1.3 degree off-axis neutrino beam. Its coordinates are N35° 43' 00" in latitude and E128° 31' 28" in longitude. The baseline from J-PARC is
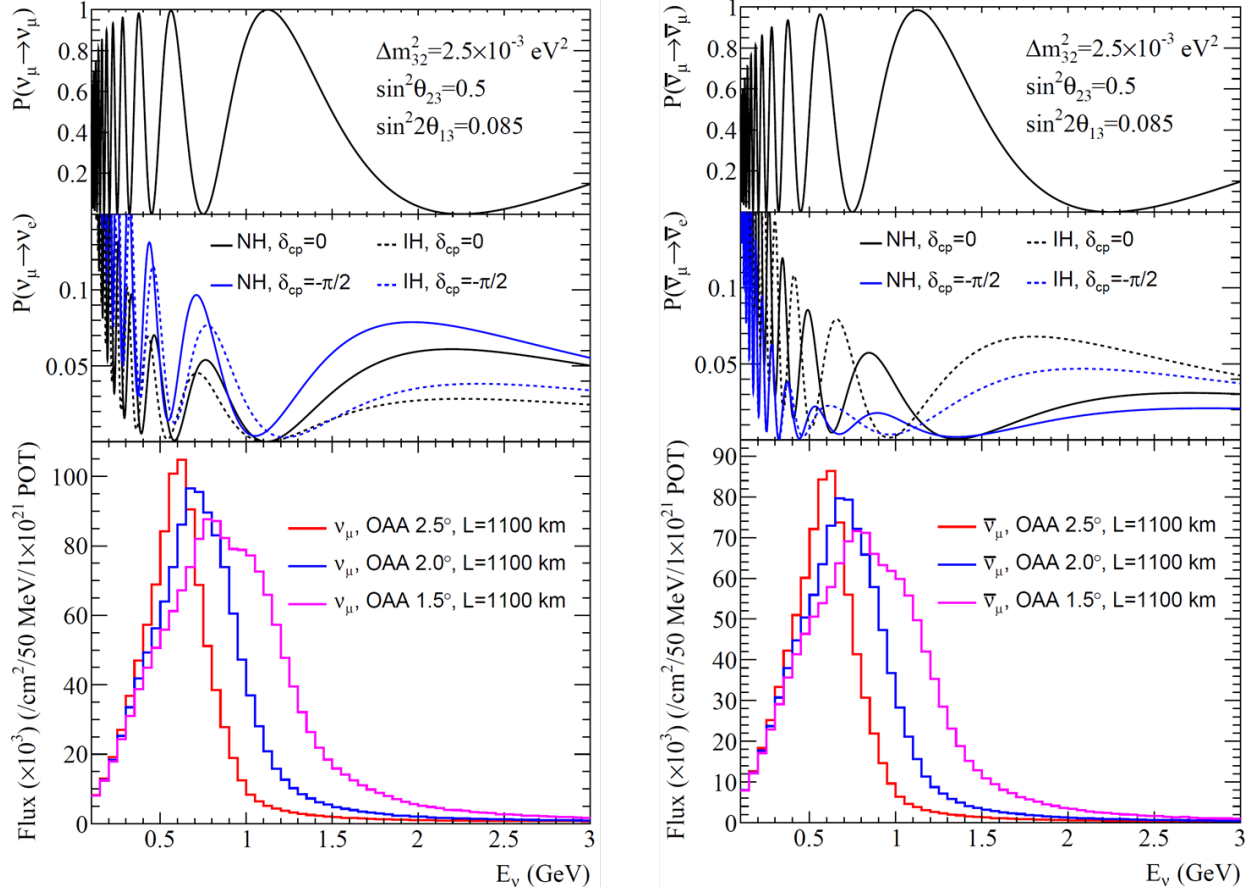
FIG. 3: Expected J-PARC neutrino (left) and antineutrino (right) spectra and oscillation probabilities at HKK assuming the baseline of 1100 km. Several off-axis angles are considered for comparison. The second oscillation maximum takes place at ∼0.6 GeV at HKK while the first one is at ∼2 GeV.

1088 km. Based on nearby ponds and rivers, sufficient underground water could be available in the site. Above all there is a traffic road including six tunnels near the Mt. Bisul that was built in October, 2014. We can take several advantages from the existing tunnels such as no hurdle in obtaining a permission for excavation, available geological-survey results, easy access of electricity lines, and easy accessibility of experimental underground facility. We find excellent access roads up to the candidate location of tunnel entrance. The HKK in the Mt. Bisul would provide a high sensitivity for the neutrino mass-ordering determination as well as an improved sensitivity for the CP phase measurement because of both first and second oscillation maxima.

The Mt. Bohyun is located at Youngcheon and holds Bohyunsan Optical Astronomy

TABLE I: Candidate sites with the off-axis angles between 1 and 2.5 degrees for the second Hyper-K detector in Korea. The baseline is the distance from the production point of the J-PARC neutrino beam.

Site	Height (m)	Baseline (km)	Off-axis angle (degree)	Elements of rock
Mt. Bisul	1084	1088	1.3°	Granite porphyry, Andesitic breccia
Mt. Hwangmae	1113	1140	1.8°	Flake granite, Porphyritic gneiss
Mt. Sambong	1186	1180	1.9°	Porphyritic granite, Biotite gneiss
Mt. Bohyun	1124	1040	2.2°	Granite, Volcanic rocks, Volcanic breccia
Mt. Minjuji	1242	1140	2.2°	Granite, Biotite gneiss
Mt. Unjang	1125	1190	2.2°	Rhyolite, Granite porphyry, Quartz porphyry

Observatory as shown in Fig. 5. The mountain is 1124 m high and made of fairly hard rocks, granite, volcanic rocks and volcanic breccia. It is an excellent candidate site for a large cavern. HKK is expected to have at least ~820 m overburden and to be exposed to a 2.2 degree off-axis neutrino beam. Its coordinates are N36° 09' 47" in latitude and E128° 58' 26" in longitude. The baseline from J-PARC is 1040 km. Based on nearby rivers, sufficient underground water is expected in the site. Its accessibility is reasonably good. The HKK in the Mt. Bohyun would make it possible to do a ratio measurement with Hyper-K and provide significant improvement for the CP-phase measurement because of the second oscillation maximum location.

In summary, we have found excellent candidate sites to build a second Hyper-K detector in Korea and to enhance the sensitivity for the CP phase and neutrino mass ordering determination. They provide larger than 800 m overburden to make additional improvement for solar neutrino measurement. The excavation cost is estimated to be reasonably low in
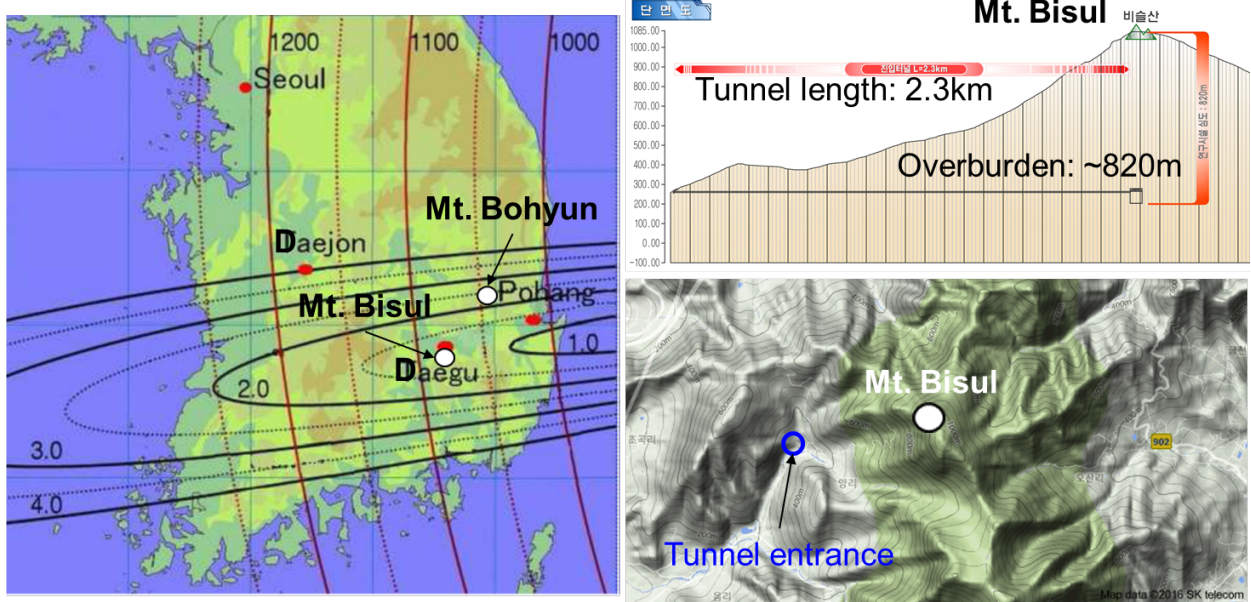
FIG. 4: Two candidate sites for the second Hyper-K detector in Korea. Mt. Bisul is located near the city of Daegu and at 1.3 degrees of off-axis angle, and Mt. Bohyun at Youngcheon and at 2.2 degrees of off-axis angle. Mt. Bisul is 1084 m high and provides excellent accessibility with an existing highway nearby. Mt. Bohyun is 1124 m high and accommodates an optical telescope on the top.

Korea.

C. Improved sensitivity from HKK

The tiny neutrino mass and the large neutrino mixing compared to quarks indicate that the origin of neutrino mass is from physics beyond the standard model, e.g. the see-saw mechanism. Tests of the unitarity of three generation neutrino mixing paradigm would provide an effective tool as demonstrated in quark mixing. Precise determination of the mixing parameters also constraints physics beyond the standard model, such as Grand Unification Theory (GUT). For example, precision measurement of CP violation phase δ_{CP} could distinguish different types of flavor symmetries in GUT as shown in Fig. 6.

The complementary information from the second detector in Korea (HKK) at different baseline length could extend the sensitivity of the overall Hyper-K significantly. Having

FIG. 5: Mt. Bohyun as a candidate site for the second Hyper-K detector in Korea. It is 1124 m high and provides ~820 m overburden for the HKK.

both HK and HKK, the J-PARC neutrino beam will provide a compelling measurement to establish CP violation measurement and improve its study of physics beyond the PMNS paradigm. Due to a factor of three enhancement of CP violation effect at the second oscillation maximum, the impact of systematic uncertainties is reduced accordingly in T2HKK. Systematic uncertainty already has significant impact on the CP sensitivity of T2K-II and it is the main limitation at T2HK. The reduction of impact from systematic uncertainty would be very important in establishing the CP violation in the neutrino oscillation. The T2HKK configuration would cover first and second oscillation maxima without serious pion production backgrounds at $E_\nu < 1$ GeV. The two different baseline oscillation measurement allows breaking the degeneracy of oscillation parameters and constrains the physics beyond
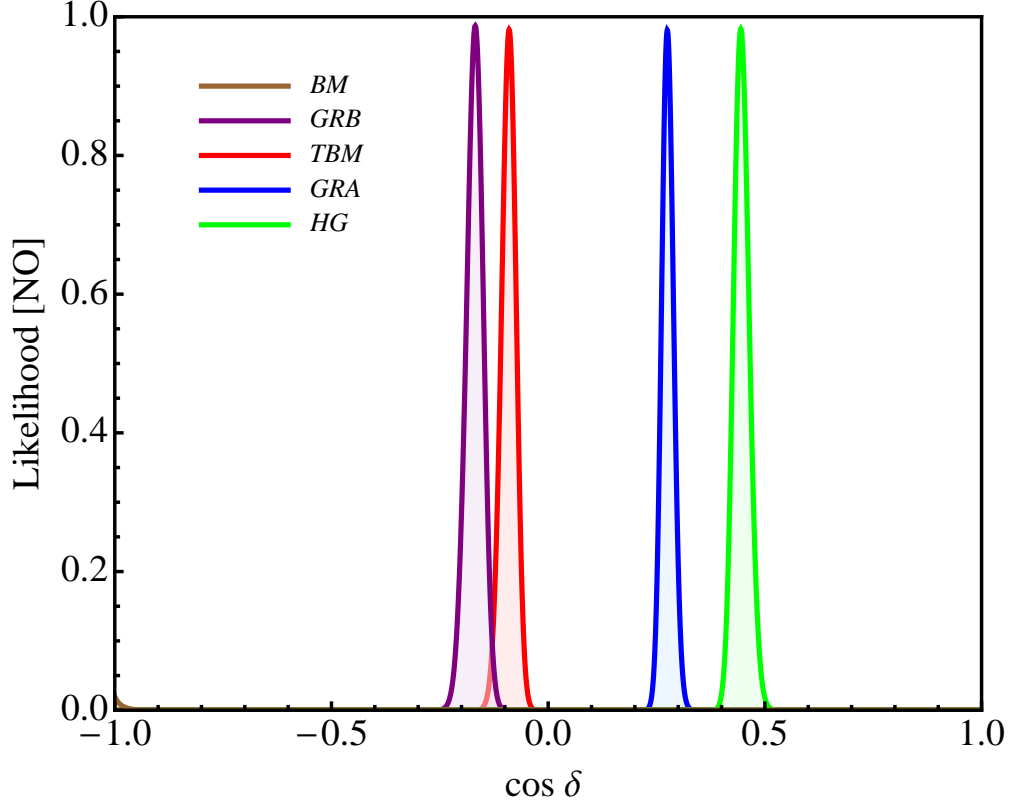
FIG. 6: The likelihood function versus $\cos \delta_{CP}$ for normal ordering neutrino mass spectrum for different types of flavor symmetries assuming the prospective 1σ uncertainties in the determination of the neutrino mixing angles [22].

PMNS paradigm. Matter effect creates a fake CP violation effect causing difference in ν and $\bar{\nu}$ oscillations. The higher energy spectrum of HKK near the first oscillation maximum, is in particular sensitive to the matter effect and expected to resolve the mass hierarchy better than 5σ level. Other degeneracies of δ_{CP} and θ_{23} octant or Δm_{31}^2 can also be constrained. Non-standard neutrino interaction can cause additional matter effect and a new physics beyond PMNS may cause distortion in oscillation pattern. Both of these effects can be tested by the two baseline T2HKK data.

In the following section, some of the quantitative studies are presented to demonstrate the impact of T2HKK on the Hyper-K project.

III. IMPROVED NEUTRINO MASS ORDERING AND CP SENSITIVITIES

This chapter describes the sensitivity to measure the neutrino mass ordering and discover CP violation using a configuration of Hyper-K with one tank in Japan and the second tank in Korea. First, the sensitivities to CP violation and the mass ordering are discussed by presenting the neutrino oscillation probability formulas and their energy dependence at a baseline to Korea, $\sim$1100 km. Then expected reconstructed event spectra for the Korean detector are presented and the effect of the oscillation parameters on these spectra are considered. The impact of systematic errors on the expected spectra are also presented. Finally, sensitivity studies for the mass ordering measurement, CP violation discovery, and precision of the CP phase measurement are presented.

A. Neutrino Oscillation Probabilities

The sensitivity enhancement of a second detector in Korea can be understood by first examining the $P(\nu_\mu \to \nu_e)$ and $P(\bar{\nu}_\mu \to \bar{\nu}_e)$ probabilities in vacuum and then examining the probabilities with the matter effect included. The approximate oscillation probability in vacuum is:

$$
\begin{aligned}
P(\nu_\mu(\bar{\nu}_\mu) \to \nu_e(\bar{\nu}_e)) \approx\ & \sin^2\theta_{23}\ \sin^2 2\theta_{13}\ \sin^2(\frac{\Delta m_{31}^2 L}{4E}) \\
& + \sin 2\theta_{23}\sin 2\theta_{13}\sin 2\theta_{12}\cos\theta_{13}\sin(\frac{\Delta m_{31}^2 L}{4E})\sin(\frac{\Delta m_{21}^2 L}{4E})\cos(\frac{\Delta m_{31}^2 L}{4E})\cos\delta \\
& - (+)\sin 2\theta_{23}\sin 2\theta_{13}\sin 2\theta_{12}\ \cos\theta_{13}\sin^2(\frac{\Delta m_{31}^2 L}{4E})\sin(\frac{\Delta m_{21}^2 L}{4E})\sin\delta \\
& + \cos^2\theta_{13}\ \cos^2\theta_{23}\ \sin^2 2\theta_{12}\ \sin^2(\frac{\Delta m_{21}^2 L}{4E}).
\end{aligned}
\tag{1}
$$

Here, the Δm_{32}^2 and Δm_{31}^2 mass splittings have been treated as equal. The first line represents the oscillations at the atmospheric mass splitting, and this term dominates for L/E values of $\sim$(500 km)/(1 GeV) typical of accelerator based long baseline oscillation experiments. The fourth line gives the oscillations through the solar mass splitting, which are small for the L/E values of interest. The second and third lines are the CP conserving and CP violating parts respectively of the interference term. The sign of the third line flips when considering antineutrinos, introducing the CP violation effect. The CP violating interference
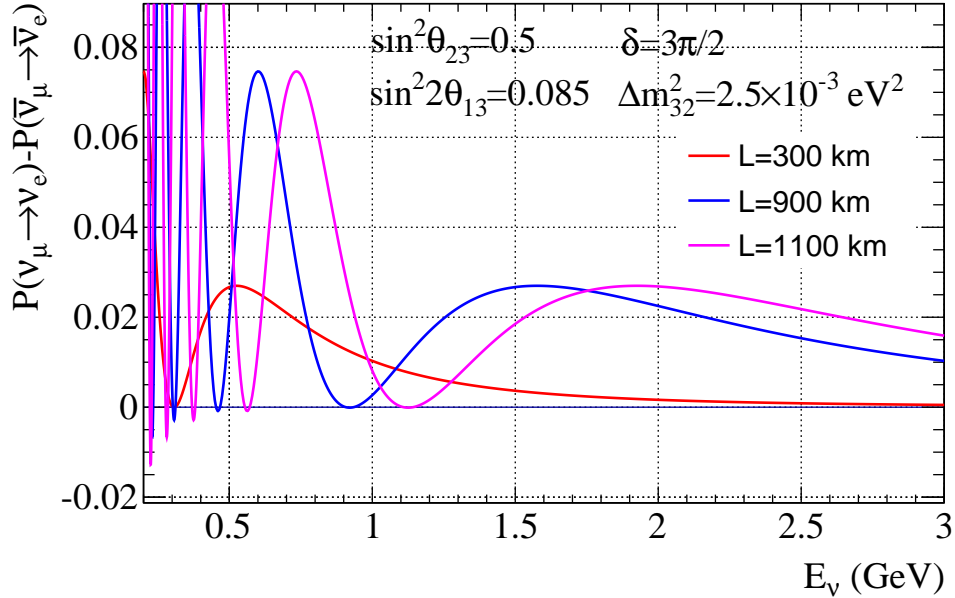
FIG. 7: The CP probability difference for $\delta = 3\pi/2$ at 300 km and 900 km baselines for oscillations in vacuum. The CP probability difference for 1100 km baseline is also shown since it is the typical baseline for candidate sites in Korea.

term depends on $\sin(\frac{\Delta m_{21}^2 L}{4E})$. Since the argument is small for the L/E values of interest, this can be expanded up to the linear term, introducing a dependence on $\frac{\Delta m_{21}^2 L}{4E}$. For a fixed energy, a larger CP effect will be observed at longer baselines. The oscillation maxima are observed when $\frac{\Delta m_{31}^2 L}{4E} = n\pi/2$ and n is an odd integer. For a fixed baseline, the second oscillation maximum will be located at 1/3 the energy of the first oscillation maximum. Or, for a fixed energy, the necessary baseline to observe the second oscillation maximum will be 3 times larger than the baseline needed to observe the first oscillation maximum. While the neutrino flux statistics will decrease by the ratio of the baselines squared, a factor of 1/9 in this case, the CP effect is 3 times larger at the second oscillation maximum, suggesting that an equally significant CP violation measurement can be made at the second oscillation maximum with a 3 times larger baseline. This is illustrated in Fig. 7 where the CP probability difference is shown for baselines of 300 km and 900 km. Since the statistics are smaller at the longer baseline, but the CP effect is larger, measurements at the second oscillation maximum may also see a smaller impact from certain systematic uncertainties.

When neutrinos propagate in matter, the matter potential is added to the Hamiltonian of the system, modifying the neutrino oscillation probabilities. The approximate oscillation probability in matter can be written as [23]:

$$
\begin{aligned}
P(\nu_\mu(\bar{\nu}_\mu) \rightarrow \nu_e(\bar{\nu}_e)) \approx{} & \sin^2\theta_{23} \ \sin^2 2\theta_{13} \frac{\sin^2(\Delta_{31} - (+)aL)}{(\Delta_{31} - (+)aL)^2} \Delta_{31}^2 \\
& + \sin 2\theta_{23}\sin 2\theta_{13}\sin 2\theta_{12}\cos\theta_{13}\frac{\sin(\Delta_{31} - (+)aL)}{(\Delta_{31} - (+)aL)}\Delta_{31}\frac{\sin(aL)}{aL}\Delta_{21}\cos(\Delta_{32})\cos\delta \\
& - (+)\sin 2\theta_{23}\sin 2\theta_{13}\sin 2\theta_{12}\cos\theta_{13}\frac{\sin(\Delta_{31} - (+)aL)}{(\Delta_{31} - (+)aL)}\Delta_{31}\frac{\sin(aL)}{aL}\Delta_{21}\sin(\Delta_{32})\sin\delta \\
& + \cos^2\theta_{13} \ \cos^2\theta_{23} \ \sin^2 2\theta_{12} \frac{\sin^2(aL)}{(aL)^2} \Delta_{21}^2.
\end{aligned}
\tag{2}
$$

Here, $\Delta_{21} = \frac{\Delta m_{21}^2 L}{4E}$ and $\Delta_{31} = \frac{\Delta m_{31}^2 L}{4E}$. The matter effect depends on $a = G_F N_e/\sqrt{2}$, where G_F is Fermi's constant and N_e is the number density of electrons in the matter. The sign of the aL terms flip for antineutrinos, introducing an effect that can mimic CP violation for some experimental configurations. It is clear from this formula that the introduction of matter effects introduces a linear dependence on Δ_{31}, allowing for the measurement of the sign of Δ_{31}, *i.e.* the mass ordering. The matter effect increases with baseline, so experiments with longer baselines will have more sensitivity to determine the mass ordering.

The (anti)neutrino oscillation probabilities for a baseline of $L = 1100$ km (a typical baseline in Korea) are shown in Fig. 8. In the region of the first oscillation maximum above 1.2 GeV, the matter effect has separated the oscillation probabilities for normal and inverted ordering for all values of the CP phase. In the region of the second oscillation maximum, 0.5-1.2 GeV, the CP probability differences are significant, while the matter effect also affects the height and position of the oscillation maximum. The spectra shapes for $1.5°$ off-axis beams are also shown for comparison. These suggest that with such a beam, it would be possible to measure the mass ordering with the high energy part of the neutrino spectrum at the first oscillation maximum, while measuring the CP phase with the second and even third oscillation maxima.
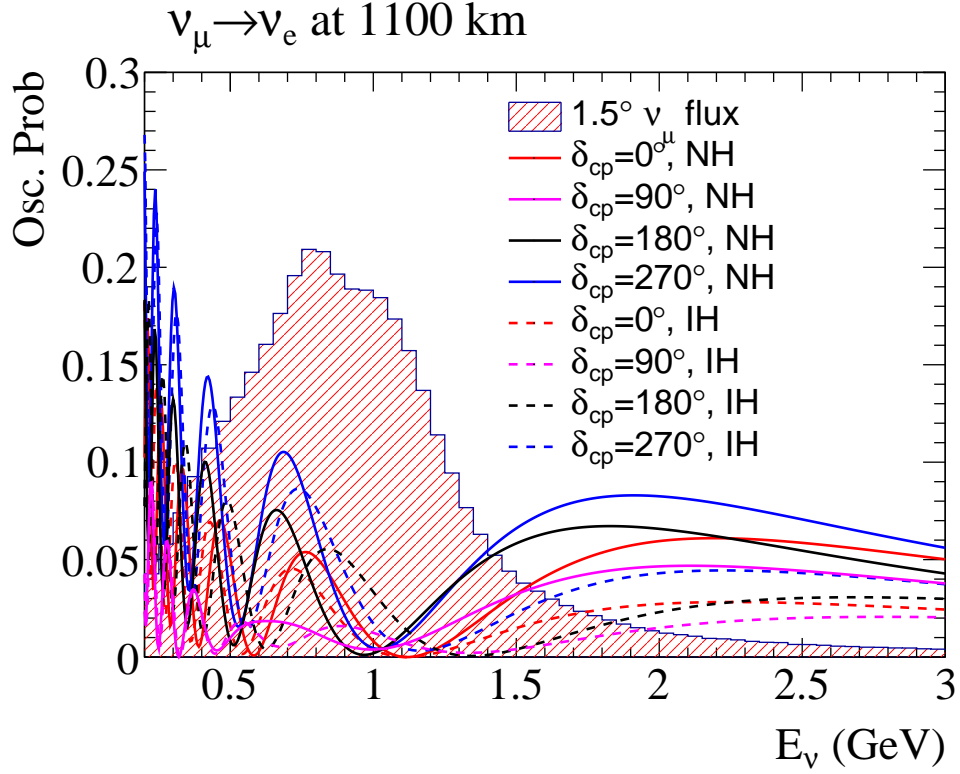
FIG. 8: The oscillation probabilities for $\delta = 0, \pi/2, \pi, 3\pi/2$ and normal and inverted mass ordering are shown for neutrinos (top) and antineutrinos (bottom). Expected muon (anti)neutrino spectra at 1.5° off-axis with arbitrary normalization are shown for comparison.

B. Event Rates at Korean Detectors

For the purpose of the sensitivity studies presented here, we consider generic detector locations in South Korea at a baseline of 1100 km and an off-axis angle of 1.5°, 2.0° or 2.5°. The expected event rates are estimated using a NEUT [24] 5.3.2-based simulation of the Super-K detector, where the fiducial mass has been scaled from 22.5 kton to 187 kton. The simulated events are scaled to give good agreement with NEUT 5.1.4.2, which has been tuned against T2K near detector data. Following the running plan of Hyper-K, an exposure of (1.3 MW)×(10×10^7 sec) is assumed with a 3:1 ratio of antineutrino mode to neutrino mode operation. Oscillation probabilities are calculated using Prob3++ [25], and a constant matter density of 3.0 g/cm^3 is assumed for the 1100 km baseline [26]. For each detector configuration, reconstructed events are classified in 4 categories:

- Neutrino mode, 1Re: Single electron-like ring candidates collected in the neutrino mode operation of the beam.

- Antineutrino mode, 1Re: Single electron-like ring candidates collected in the antineutrino mode operation of the beam.

- Neutrino mode, 1Rμ: Single muon-like ring candidates collected in the neutrino mode operation of the beam.

- Antineutrino mode, 1Rμ: Single muon-like ring candidates collected in the antineutrino mode operation of the beam.

The selection cuts for these candidate samples are identical to the selection cuts used in recent T2K oscillation measurements [27], except for the reconstructed energy, E_{rec} <1.25 GeV cut on the 1Re samples. This cut has been removed since the matter effect which constrains the mass ordering is most strongly manifested in events with reconstructed energy greater than 1.25 GeV.

Predicted event rates for normal mass ordering and δ_{cp}=0 are shown for 1Re and 1Rμ samples in Fig. 9/Table II and Fig. 10/Table III respectively. In Tables II, III, the predicted event rates for the nominal Hyper-K tank location are shown for comparison. These differ from those presented in the Hyper-K Design Report since the value for $\sin^2\theta_{13}$ has been updated to the 2015 PDG value, a new version of NEUT is used for the neutrino interaction

TABLE II: The expected number of ν_e and $\bar{\nu}_e$ 1Re candidate events. Normal mass ordering with $\sin^2 2\theta_{13} = 0.085$ and $\delta_{cp} = 0$ are assumed. Background is categorized by the flavor before oscillation.

Detector Location	Signal	Wrong-sign Signal	Intrinsic ν_e, $\bar{\nu}_e$	NC	CC ν_μ,$\bar{\nu}_\mu$	Total
OAA, L			Neutrino Mode			
2.5°, 295 km	1426.1	15.4	269.3	125.0	7.1	1842.9
2.5°, 1100 km	87.9	1.7	28.3	12.5	1.7	132.2
2.0°, 1100 km	122.6	2.0	33.8	21.4	2.4	182.3
1.5°, 1100 km	140.6	2.4	39.1	39.1	3.7	224.8
OAA, L			Antineutrino Mode			
2.5°, 295 km	1053.1	164.3	338.3	153.5	4.2	1713.4
2.5°, 1100 km	89.8	15.5	39.4	14.3	0.8	159.8
2.0°, 1100 km	131.5	19.8	46.3	23.4	1.1	222.1
1.5°, 1100 km	159.1	23.9	54.3	39.5	1.7	278.5

generation, and a 10 year exposure with one tank is presented here, while the Design Report assumes a 10 year exposure with one tank for the first 6 years and a second tank for the remaining 4 years. The 1Re candidate rates in Korea are $\sim 1/10$ the rates at the 295 km baseline due to the $1/L^2$ dependence of the flux. In the 1Rμ samples, the first and second oscillation maxima can be observed at 2 GeV and 0.7 GeV respectively.

The variations of the 1Re spectra in neutrino mode and antineutrino mode for different δ_{cp} values at different detector locations are shown in Fig. 11. Similarly, the asymmetries of predicted 1Re spectra between neutrino mode and antineutrino mode as a function of δ_{cp} are shown in Fig. 12. For the detectors in Korea, the magnitude of the potential neutrino/antineutrino asymmetry is larger and this effect can partially compensate for the larger statistical uncertainties at the 3.7 times longer baseline. The purely statistical separations between the maximally CP violating and CP conserving hypotheses are listed in Table IV, where it is assumed that the mass ordering is known. The 2.0° off-axis slice has the strongest statistical separation between CP violating and CP conserving hypotheses.

FIG. 9: Predicted 1Re candidate rates for neutrino mode (left) and antineutrino mode (right) with the detector at a 1.5° (top), 2.0° (middle) or 2.5° (bottom) off-axis angle. The oscillation parameters are set to δ_{cp}=0, $\Delta m^2_{32} = 2.5 \times 10^{-3}$ eV^2 (normal mass ordering), $\sin^2\theta_{23}$=0.5, $\sin^2\theta_{13}$=0.0219.
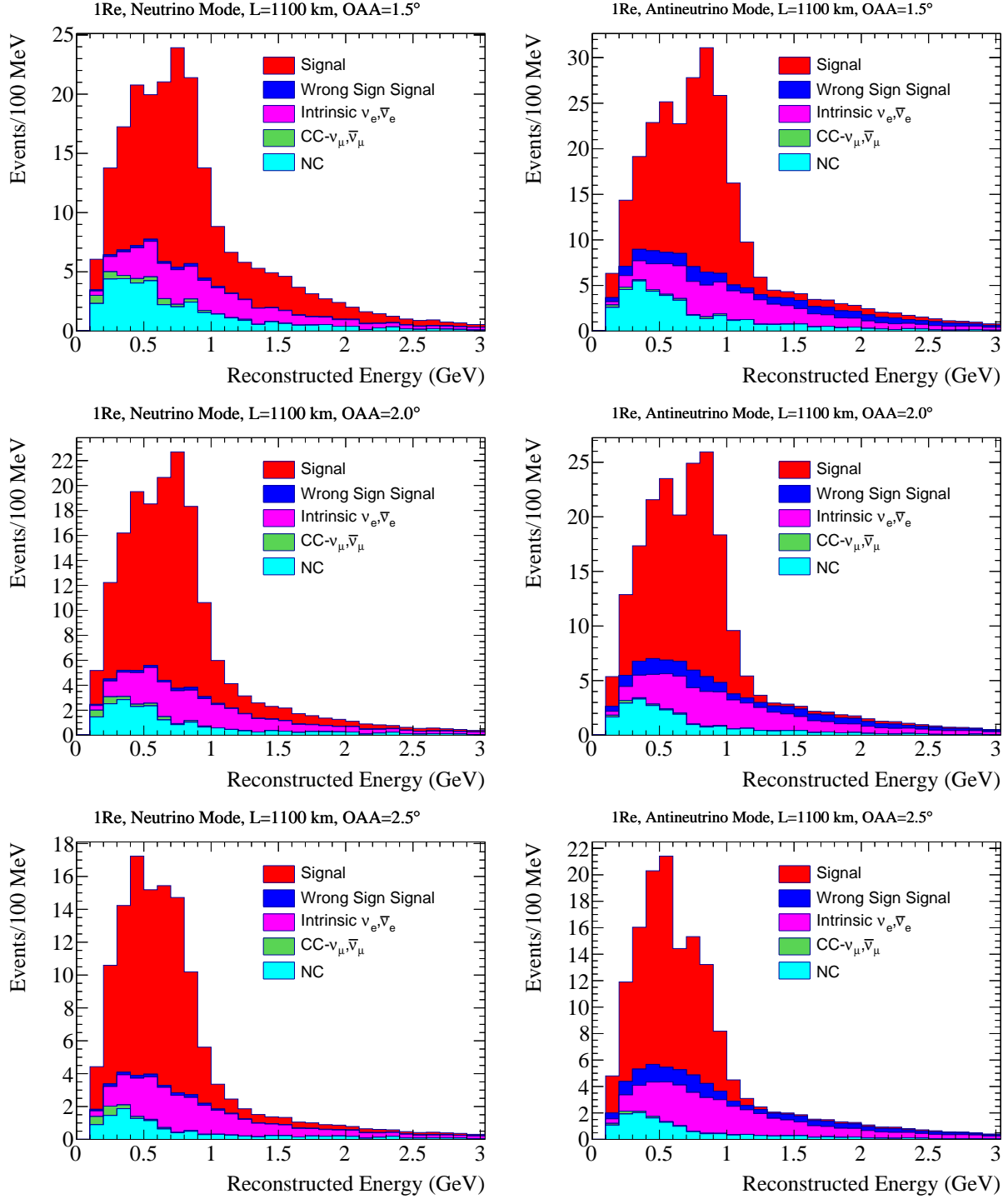
FIG. 10: Predicted 1Rμ candidate rates for neutrino mode (left) and antineutrino mode (right) with the detector at a 1.5° (top), 2.0° (middle) or 2.5° (bottom) off-axis angle. The oscillation parameters are set to δ_{cp}=0, $\Delta m^2_{32} = 2.5 \times 10^{-3}$ eV^2 (normal mass ordering), $\sin^2\theta_{23}$=0.5, $\sin^2\theta_{13}$=0.0219.
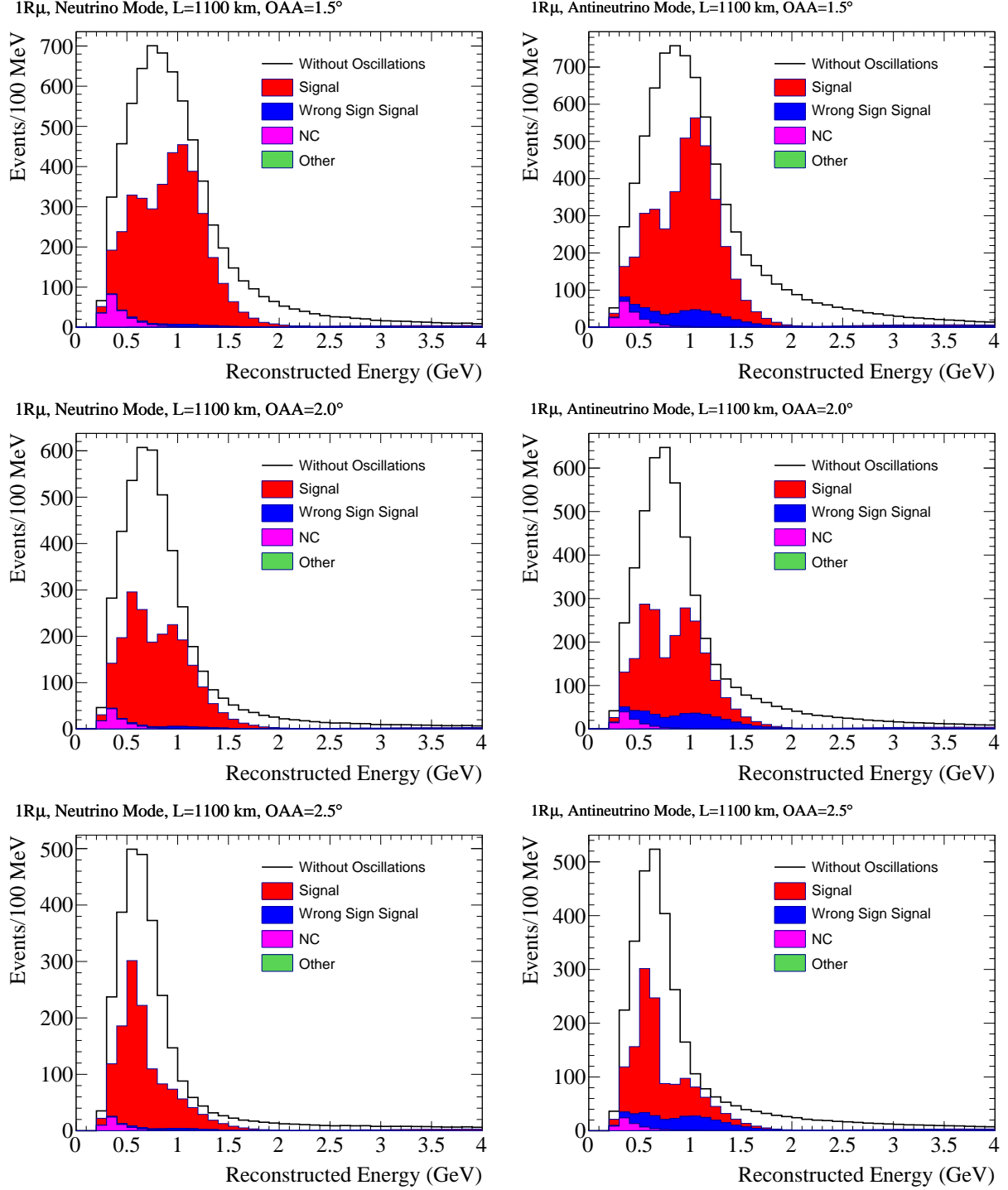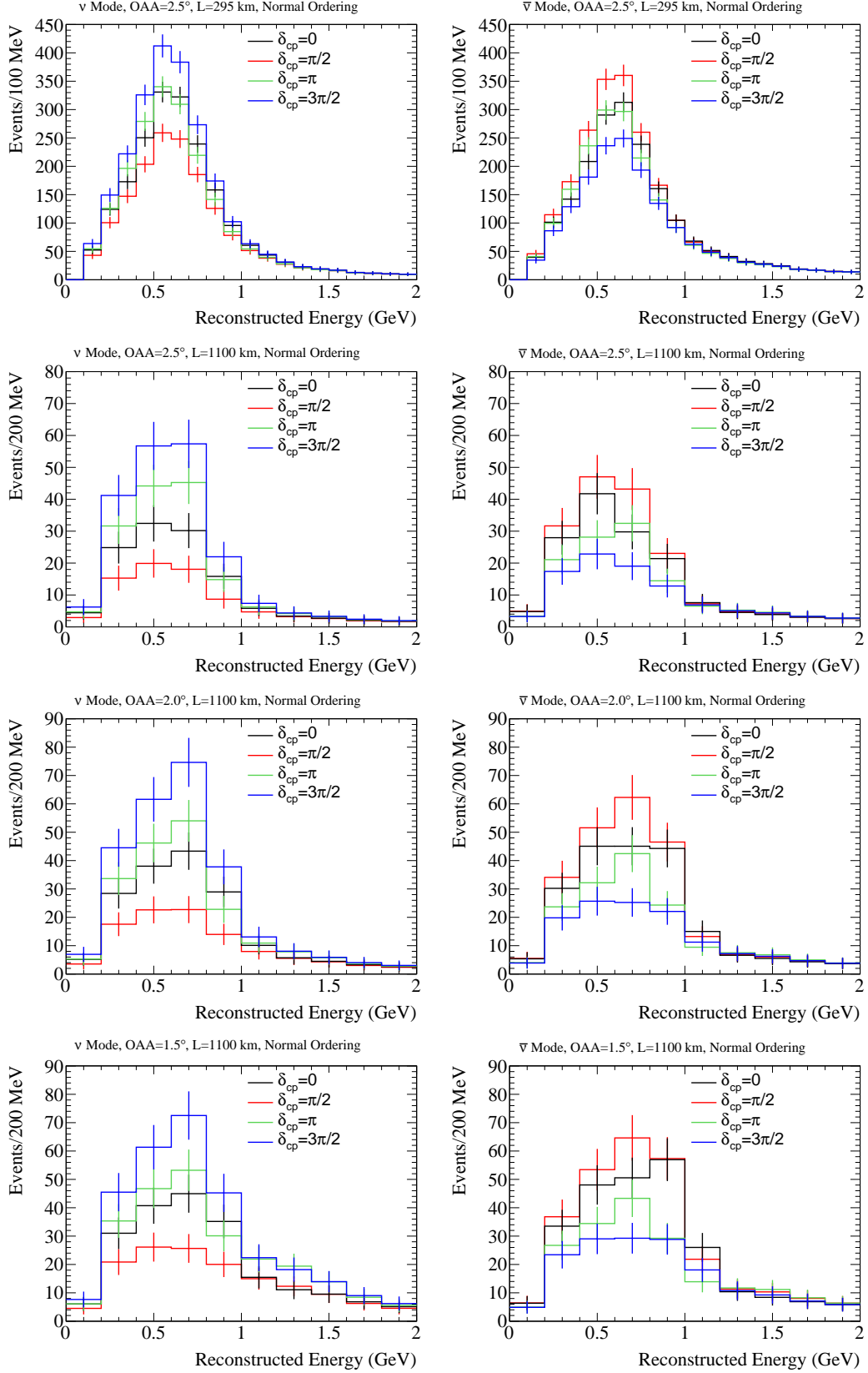
FIG. 11: The predicted 1Re spectra in neutrino mode (left) and antineutrino mode (right) for different values of δ_{cp}.

TABLE III: The expected number of ν_μ and $\bar{\nu}_\mu$ 1Rμ candidate events. Normal mass ordering with $\sin^2\theta_{23} = 0.5$ and $\Delta m^2_{32} = 2.5 \times 10^{-3}$ eV^2 are assumed

Detector Location	Signal	Wrong-sign Signal	NC	CC-ν_e,$\bar{\nu}_e$	Total
OAA, L		Neutrino Mode			
2.5°, 295 km	9062.5	571.2	813.6	29.5	10476.9
2.5°, 1100 km	1275.0	32.7	58.5	1.9	1368.1
2.0°, 1100 km	2047.2	42.8	107.7	2.5	2200.2
1.5°, 1100 km	3652.0	55.4	210.4	2.9	3920.7
OAA, L		Antineutrino Mode			
2.5°, 295 km	8636.1	4905.9	860.8	23.6	14426.5
2.5°, 1100 km	1119.5	300.6	61.9	2.0	1484.0
2.0°, 1100 km	1888.5	390.0	102.6	2.4	2384.4
1.5°, 1100 km	3579.2	490.8	185.1	2.8	4257.9

TABLE IV: The statistical separation of the predicted maximally CP violating spectra from the predicted CP conserving spectrum. Here the significance is calculated for both CP conserving hypotheses and the smallest significance is shown. The mass ordering is assumed to be known.

Detector Location	Significance (σ)			
	NH		IH	
OAA, L	$\delta_{cp} = \pi/2$	$\delta_{cp} = 3\pi/2$	$\delta_{cp} = \pi/2$	$\delta_{cp} = 3\pi/2$
2.5°, 295 km	11.6	11.0	11.8	10.9
2.5°, 1100 km	6.1	4.9	6.5	4.9
2.0°, 1100 km	7.9	5.9	7.1	6.3
1.5°, 1100 km	6.9	5.3	5.9	5.7

The impact of the matter effect and sensitivity to mass ordering is illustrated in Fig. 13. Here, a double difference is presented. First the difference in observed neutrino mode and antineutrino mode 1Re candidates is calculated as a function of reconstructed energy. This
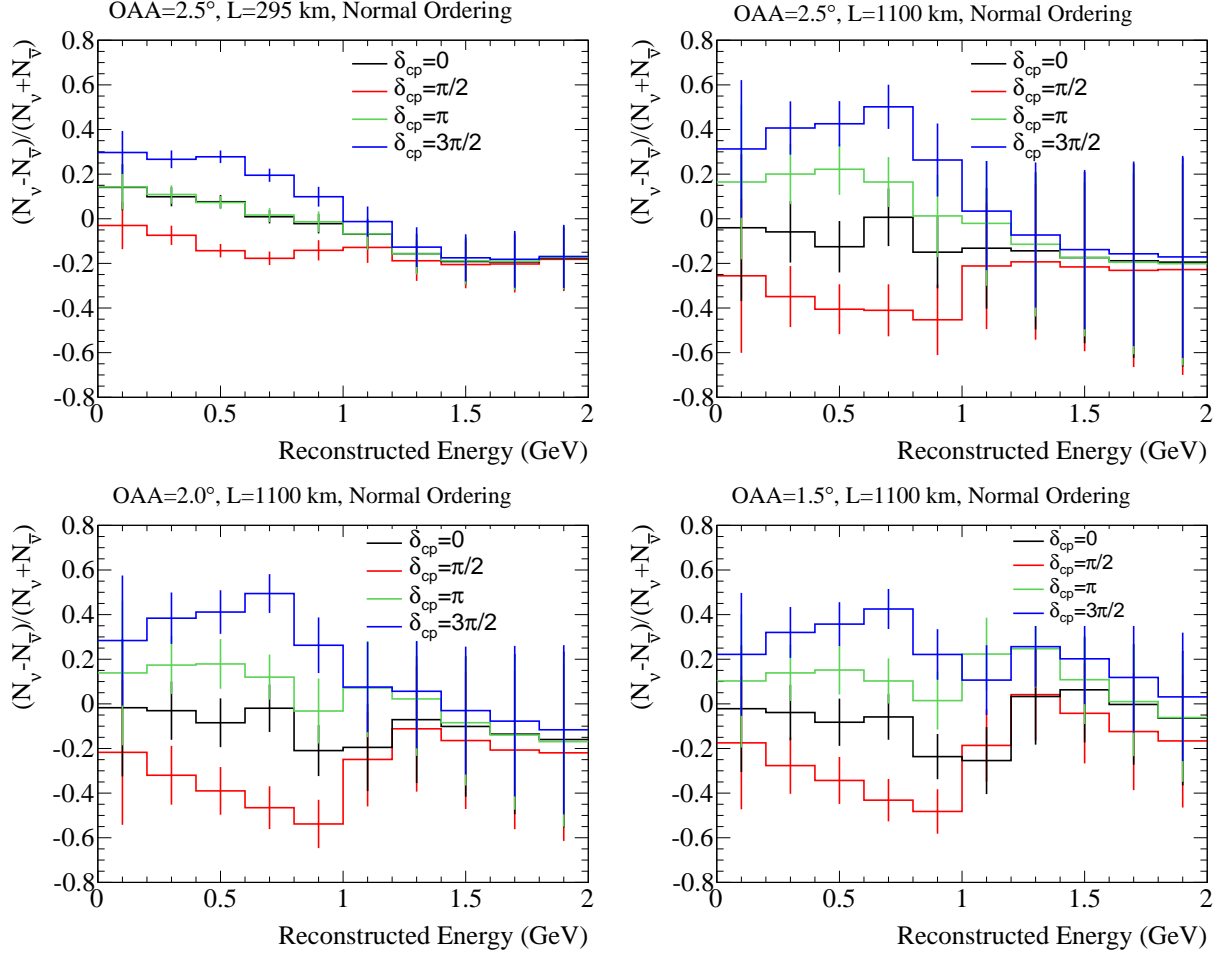
FIG. 12: The event rate asymmetry between neutrino mode and antineutrino mode for variations of δ_{cp} at different detector site locations.

difference is calculated for both the normal and inverted hierarchies and the difference between hierarchies is taken. It can be seen that the neutrino-antineutrino difference varies differently with reconstructed energy for normal and inverted hierarchies. For the normal mass ordering, the neutrinos are enhanced in the < 0.8 GeV and > 1.1 GeV regions and diminished in the 0.8-1.0 GeV region relative to the inverted mass ordering. This relative difference is nearly independent of the true value of δ_{cp}, as illustrated in Fig. 13. The 1.5° off-axis angle configuration allows for a significant observation of this spectral dependence of the asymmetry in the 0.8-1.0 GeV and > 1.1 GeV regions. The 2.0° off-axis angle configuration has little sensitivity to the > 1.1 GeV region, and the 2.5° off-axis configuration is only sensitive to the < 0.8 GeV region.
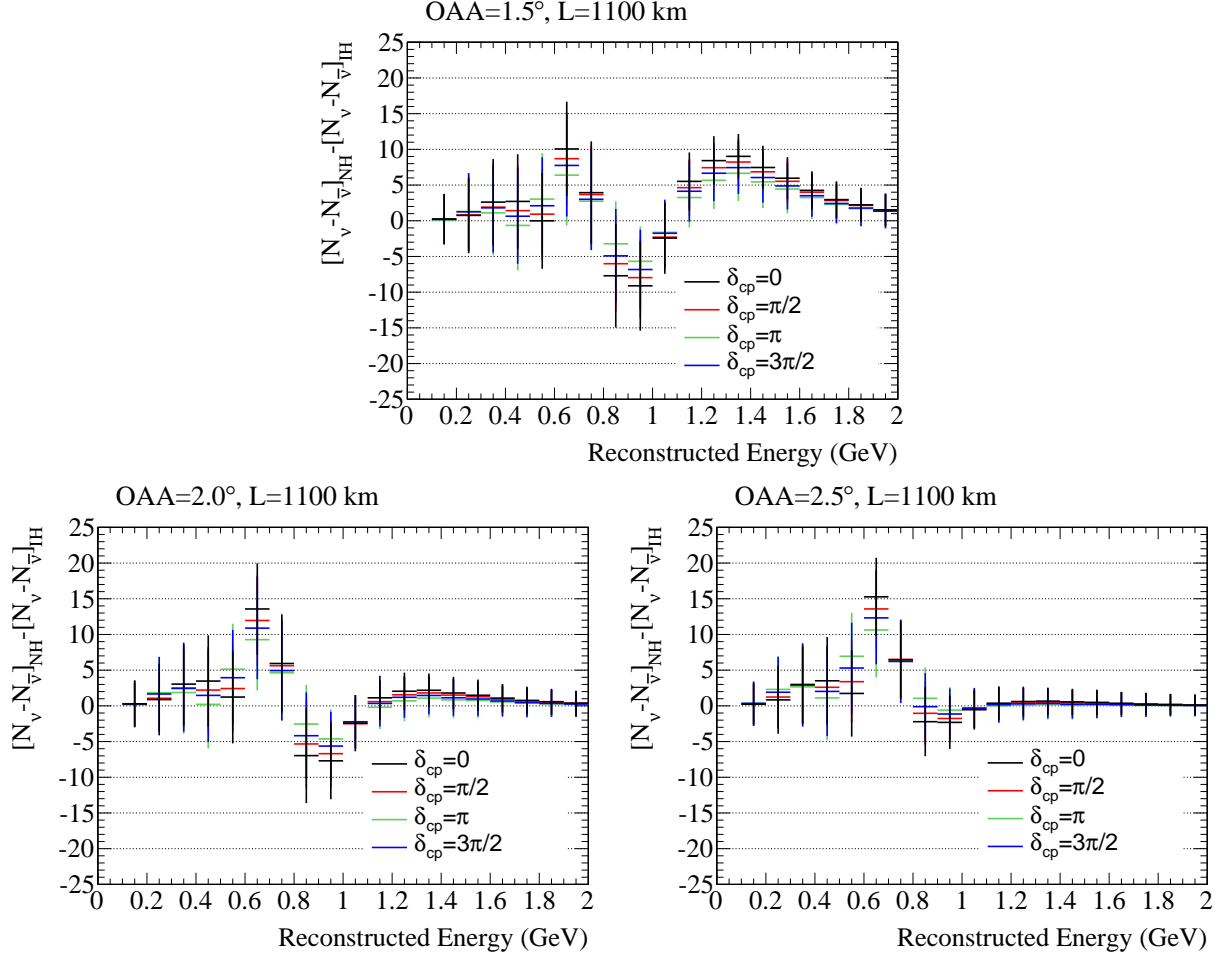
FIG. 13: The difference of the observed neutrino-antineutrino difference in the 1Re samples for normal mass ordering relative to the expected differences for inverted mass ordering. Error bars are the propagated statistical errors for the neutrino mode and antineutrino mode 1Re samples.

While the CP-even and CP-odd interference terms in the electron (anti)neutrino appearance probability are enhanced at the 1100 km baseline due to the Δ_{21} dependence, no such enhancement is present in the muon (anti)neutrino survival probability. Hence, the statistical constraint from the 1Rμ samples on Δm^2_{32} and $\sin^2 2\theta_{23}$ will be stronger for the detector at $L = 295$ km due to the larger statistics. The Korean detector, however, has the unique feature of measuring the oscillation pattern over two periods, confirming the oscillatory behavior of the neutrino transitions. Fig. 14 shows the ratio of the expected spectrum after oscillations to the expected spectrum without oscillations. For all three Korean detector locations, the oscillation pattern over two periods may be observed. While the measurement

30

in Hyper-K provides higher statistics, only one period of oscillations can be observed.
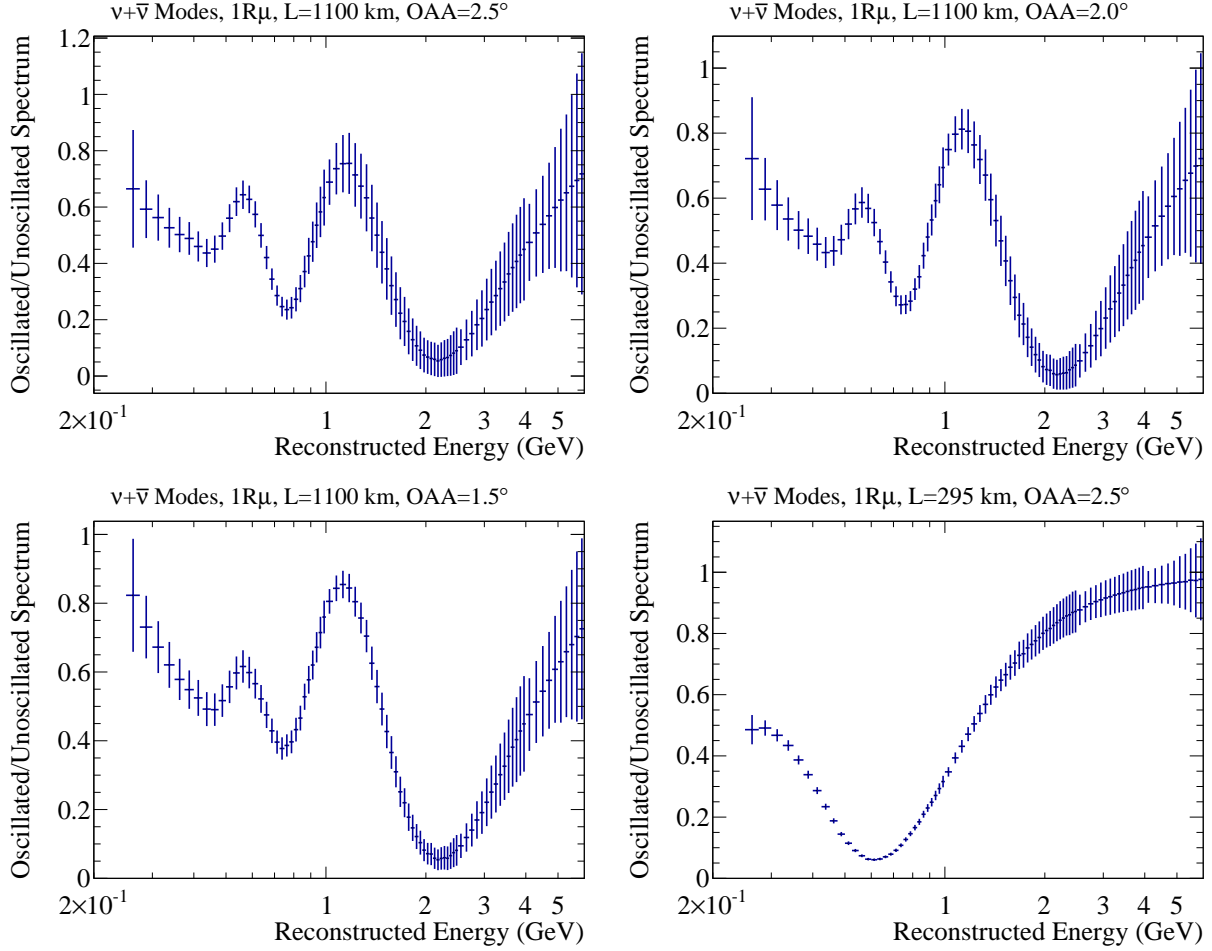

FIG. 14: The ratio of the predicted $1R\mu$ spectrum with oscillations to the predicted $1R\mu$ spectrum without oscillations. Here, the neutrino mode and antineutrino mode data have been summed. The bin width varies from 25 MeV at low energy to 100 MeV at high energy, and the errors on each bin represent the statistical error for that bin.

C. Systematic Errors

Due to the statistically large samples available in the Hyper-K experiment, systematic errors are likely to represent the ultimate limit on oscillation parameter measurement precision. An advantage of a Korean detector is to enhance the contribution of the δ_{cp} dependent interference terms at the cost of fewer statistics, achieving similar sensitivity in a statistics

limited measurement. To evaluate the impact of the Korean detector on the Hyper-K sensitivities, it is necessary to implement a systematic error model that takes into account what are expected to be the dominant systematic errors for Hyper-K. The systematic error model should also account for any new systematic errors introduced by having a detector in Korea. The systematic errors considered for the sensitivity studies presented in this paper are:

- $\sigma_{\nu_e}/\sigma_{\nu_\mu}$ **and** $\sigma_{\bar{\nu}_e}/\sigma_{\bar{\nu}_\mu}$ - The interaction cross sections for ν_e and $\bar{\nu}_e$ are not currently precisely measured with near detector data, although they may be more precisely measured in the Hyper-K era. When extrapolating the measured ν_μ and $\bar{\nu}_\mu$ rates from the near detectors, it is necessary to assign and uncertainty on the interaction cross section ratios $\sigma_{\nu_e}/\sigma_{\nu_\mu}$ and $\sigma_{\bar{\nu}_e}/\sigma_{\bar{\nu}_\mu}$. Here the T2K approach based on the work of Day & McFarland [28] is taken. Separate normalization parameters are assigned to vary σ_{ν_e} and $\sigma_{\bar{\nu}_e}$. The correlation between these parameters is assigned assuming there is a 2% systematic effect that is uncorrelated between neutrinos and antineutrinos and an additional 2% systematic effect with anticorrelation between neutrinos and antineutrinos.

- **Energy scale at the far detectors** - The energy scale at Super-K is calibrated using samples of Michel electrons, π^0s and stopping cosmic muons. In T2K oscillation analyses, the energy scale error is found to be 2.4% [27]. Here a 2.4% energy scale uncertainty is applied to the reconstructed energy for events in Hyper-K and the Korean detector. Independent parameters with no correlation are used for Hyper-K and the Korean detector. 100% correlation between the 1Rμ and 1Re samples is assumed.

- **Matter density** - For results presented here, a constant matter density of 3.0 g/cm^3 is assumed for the path to the Korean detector. An uncertainty of 6% is assigned based on previous estimates [26].

- **The NCπ^+ background** - NCπ^+ interactions are a significant background in the 1Rμ samples. Based on the approach taken by T2K [27], a 30% error is applied here.

- **The intrinsic $\nu_e(\bar{\nu}_e)$ and NCπ^0 backgrounds** - The backgrounds for the 1Re samples are the intrinsic $\nu_e(\bar{\nu}_e)$ in the beam and NCπ^0 interactions mistaken for an electron. It is expected that these backgrounds will be measured by an intermediate water

Cherenkov detector with similar $\nu_e(\bar{\nu}_e)$ and total fluxes to the far detector fluxes. Studies of this measurement with the NuPRISM detector show an expected statistical error of 3%. A total error of 5% is considered to account for uncertainties in the different efficiency and fluxes between the near and far detectors. 100% correlation is assumed between Hyper-K and the Korean detector, but no correlation is assumed between the neutrino and antineutrino beam modes.

- **The CC non-quasielastic fraction** - The fraction of non-quasielastic interactions in the candidates samples affects the predicted normalization and reconstructed energy distribution. In T2K near detector fits, the normalization of the non-quasielastic 2p-2h component of the cross section is fitted with a 20% error. Here a 20% error is applied to the normalization of the non-quasielastic interactions. An anticorrelated parameter is applied to the quasielastic interactions, and its error is chosen such that the normalization of the unoscillated event rate is conserved for variations of these parameters. This approach models the effect of the near detector constraint.

- **Near to far extrapolation** - The T2K oscillation analysis [27] includes an uncertainty from the flux and cross section model parameters that are constrained by near detector data. This error includes the near detector measurement error and extrapolation uncertainties in the flux and cross section models that arise due to different neutrino spectra at the near and far detectors. In principle, the extrapolation error includes the effect of the previously described uncertainty on the non-quasielastic fraction. To model this uncertainty, the T2K errors are applied as an overall uncertainty on the charged current event rate. To avoid double counting the error on the non-quasielastic fraction, the T2K errors are corrected by subtracting in quadrature the normalization uncertainty that is explicitly calculated from the non-quasielastic uncertainty.

- **Far detector modeling** - In addition to the energy scale uncertainty, there are uncertainties related to the modeling of efficiencies in the far detector. This uncertainty is estimated based on the uncertainty evaluated for T2K. Since the far detector efficiency model is tuned using atmospheric neutrino control samples, it is assumed that the uncertainty will be reduced with the larger sample of atmospheric neutrinos available in Hyper-K. For the studies presented here, the assumption is that 50% of the error is

reduced by a factor of $1/\sqrt{8.3}$, where 8.3 is the fiducial mass ratio between Hyper-K and Super-K. The remaining 50% of the error remains unchanged under the assumption the perfect agreement between the detector model and control samples may not be achieved and systematic errors may be applied to cover any disagreement. For this error source, there are no correlations between Hyper-K and the Korean detector.

For the purpose of this document, the above systematic error model is used in place of the model adopted for the Hyper-K Design Report. This is done because the systematic errors used in the Hyper-K design report are based on the T2K systematic error estimate for a $2.5°$ off-axis angle flux and a 1Re sample with a $E_{rec} < 1.25$ GeV cut applied. The T2K systematic error model has not yet been applied to the other off-axis angle positions and 1Re samples with the reconstructed energy cut removed.

The effect of systematic errors propagated to the normalization uncertainties on the 1Rμ and 1Re samples are summarized in Table V. The normalization uncertainties for individual samples are in the 4-5% range. These uncertainties are slightly more conservative than those presented in the Hyper-K design report, which included a total systematic error between 3% and 4% depending on the sample. The uncertainties for the more on-axis detector locations appear marginally smaller because the broader spectrum tends to average over shape uncertainties more. The fractional uncertainties as a function of reconstructed energy are shown in Fig. 15. Here, the most prominent feature is the large uncertainty in the 1-3 GeV region of the 1Rμ samples for the detector at $L = 1100$ km. This energy range is the location of the first oscillation maximum and the large uncertainty arises from energy scale and non-quasielastic fraction uncertainties that can cause feed-down or feed-up (in the case of energy scale) into the region of the oscillation maximum.

The relationship between systematic uncertainties and the physics sensitivity with a Korean detector can be better understood by investigating a specific measurement, the precision measurement of δ_{cp} when δ_{cp} is near a maximally CP violating value of $\pi/2$ or $3\pi/2$. Near these values, the derivative of $\sin(\delta_{cp})$ approaches zero, degrading the sensitivity to the CP odd term in the oscillation probability. Here, the CP even term, which depends on $\cos(\delta_{cp})$ may contribute to the precision measurement of the phase. Fig. 16 shows the changes to the spectra for a change in a δ_{cp} by $+13°$ from an initial value of $\pi/2$ for the Hyper-K detector. Here, $13°$ is chosen since it is expected to be the ultimate precision of Hyper-K

after a 10 year×1.3 MW exposure with 2 tanks. It can be seen that the change to δ_{cp} by 13° largely effects the spectrum through the $\cos(\delta_{cp})$ term, causing a downward shift in energy with little change to the overall normalization. Fig. 16 also shows the effect of an energy scale shift by -0.5% for comparison. The energy scale shift has a similar effect on the spectrum, indicating that even a 0.5% uncertainty on the energy scale can degrade the δ_{cp} precision near maximally CP violating values. The Korean detector is constraining δ_{cp}
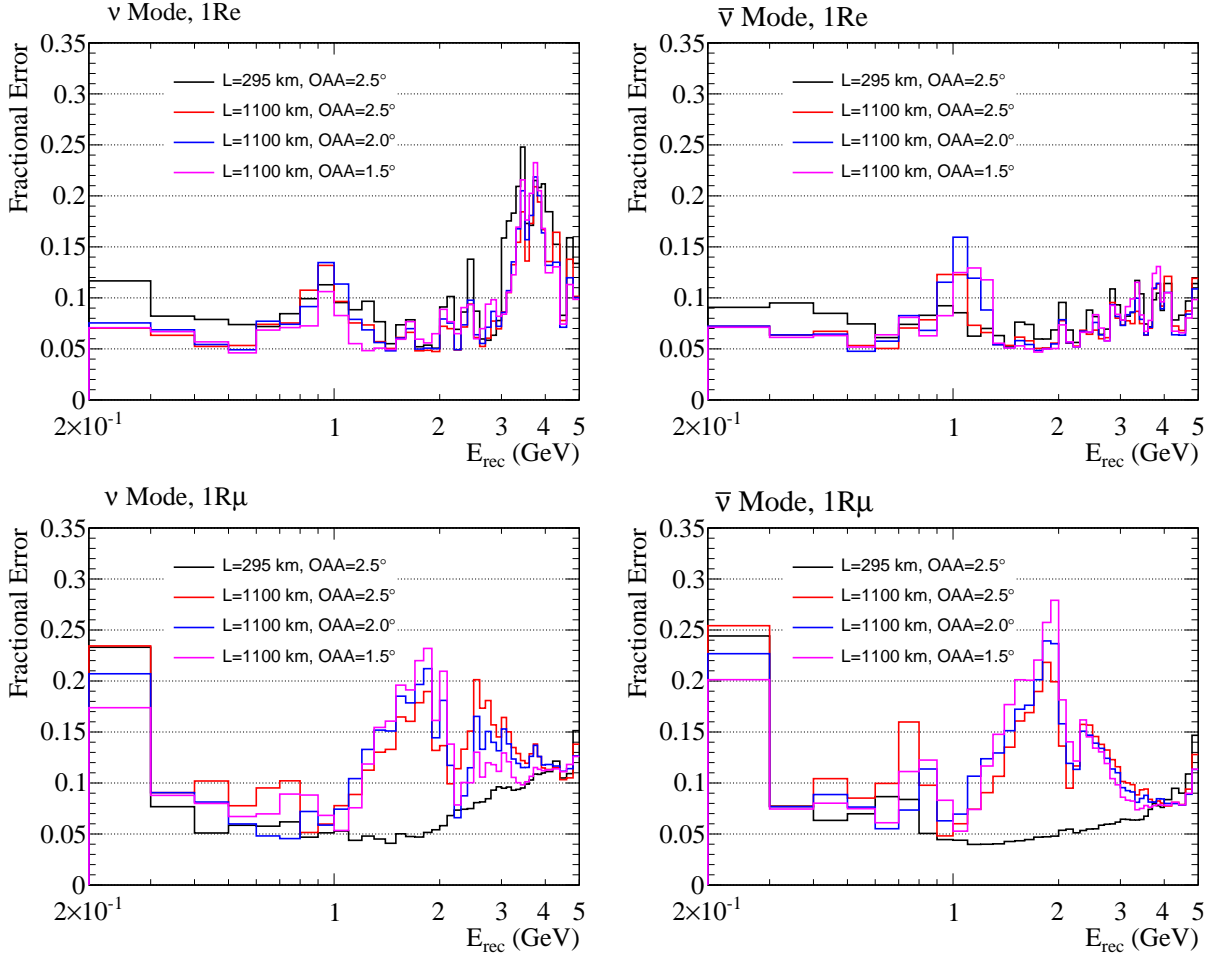

FIG. 15: The fractional systematic errors per bin on the predicted spectra binned in reconstructed energy.

with a significant number of events at the second and third oscillation maximum. Here, the effect of the interference terms in the oscillation probability is 3 times larger, and for the same shift in δ_{cp}, the CP-odd effect may be observable. Fig 17 shows the spectrum ratios for the Korean detector at 1100 km baseline and 1.5° off-axis. Here, the effect of both the

TABLE V: Percent error on the normalization of the predicted 1Rμ and 1Re samples in neutrino and antineutrino mode for each systematic error source. The error on the ratio of neutrino mode to antineutrino mode is also shown for 1Re since this uncertainty is relevant for the detection of a CP asymmetry.

| Error Source	Percent Error (%)				
	ν 1Rμ	$\bar{\nu}$ 1Rμ	ν 1Re	$\bar{\nu}$ 1Re	(ν 1Re)/($\bar{\nu}$ 1Re)
OAA=2.5°, $L = 1100$ km					
$\sigma_{\nu_e}/\sigma_{\nu_\mu}$, $\sigma_{\bar{\nu}_e}/\sigma_{\bar{\nu}_\mu}$	0.00	0.00	2.10	1.68	3.12
Energy Scale	0.02	0.02	0.01	0.01	0.01
Matter Density	0.04	0.08	0.43	0.09	0.53
NCπ^+ Bgnd.	1.28	1.25	0.00	0.00	0.00
ν_e & NCπ^0 Bgnd.	0.00	0.00	1.32	1.41	1.88
CC non-QE Fraction	2.76	1.88	1.98	1.29	2.35
Extrapolation	2.70	2.60	2.44	3.06	1.95
Far Detector Model	2.64	2.64	2.08	2.08	0.00
Total	4.69	4.16	4.54	4.47	4.86
OAA=2.0°, $L = 1100$ km					
$\sigma_{\nu_e}/\sigma_{\nu_\mu}$, $\sigma_{\bar{\nu}_e}/\sigma_{\bar{\nu}_\mu}$	0.00	0.00	2.01	1.67	3.07
Energy Scale	0.02	0.01	0.01	0.01	0.01
Matter Density	0.02	0.06	0.55	0.12	0.67
NCπ^+ Bgnd.	1.47	1.29	0.00	0.00	0.00
ν_e & NCπ^0 Bgnd.	0.00	0.00	1.26	1.29	1.76
CC non-QE Fraction	0.87	0.82	1.24	0.76	1.51
Extrapolation	2.68	2.68	2.38	3.00	1.92
Far Detector Model	2.64	2.64	2.08	2.08	0.00
Total	3.89	3.83	4.18	4.27	4.39
OAA=1.5°, $L = 1100$ km					
$\sigma_{\nu_e}/\sigma_{\nu_\mu}$, $\sigma_{\bar{\nu}_e}/\sigma_{\bar{\nu}_\mu}$	0.00	0.00	1.72	1.41	2.67
Energy Scale	0.01	0.01	0.01	0.01	0.01
Matter Density	0.01	0.06	0.24	0.28	0.53
NCπ^+ Bgnd.	1.61	1.30	0.00	0.00	0.00
ν_e & NCπ^0 Bgnd.	0.00	0.00	1.42	1.37	1.93
CC non-QE Fraction	0.44	0.30	0.52	0.37	0.75
Extrapolation	2.67	2.60	2.23	2.88	1.84
Far Detector Model	2.64	2.64	2.08	2.08	0.00
Total	3.83	3.81	3.84	4.11	3.91
OAA=2.5°, $L = 295$ km					
$\sigma_{\nu_e}/\sigma_{\nu_\mu}$, $\sigma_{\bar{\nu}_e}/\sigma_{\bar{\nu}_\mu}$	0.01	0.00	2.44	1.82	3.53
Energy Scale	0.04	0.03	0.42	0.63	0.21
Matter Density	–	–	–	–	–
NCπ^+ Bgnd.	2.33	1.79	0.00	0.00	0.00
ν_e & NCπ^0 Bgnd.	0.00	0.00	0.94	1.22	1.51
CC non-QE Fraction	1.68	1.72	2.07	1.00	2.25
Extrapolation	2.60	2.56	2.51	3.05	1.96
Far Detector Model	2.64	2.64	2.08	2.08	0.00
Total	4.13	4.15	4.71	4.47	4.90
OAA=2.5°, $L = 295$ km (Hyper-K Design Report)					
Total	3.6	3.6	3.2	3.9	–
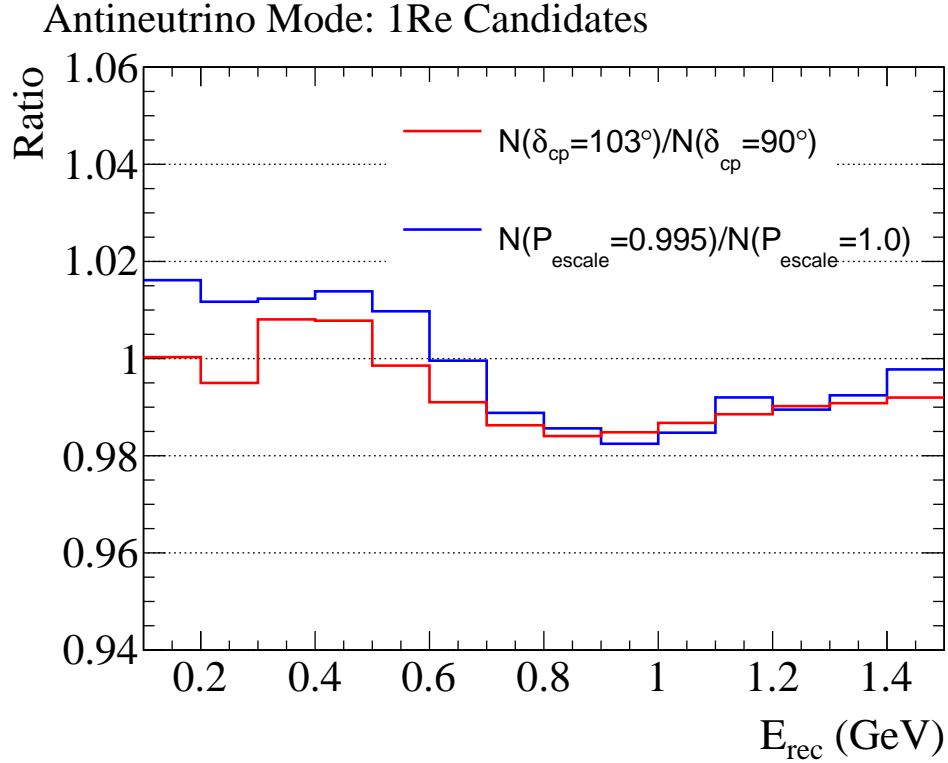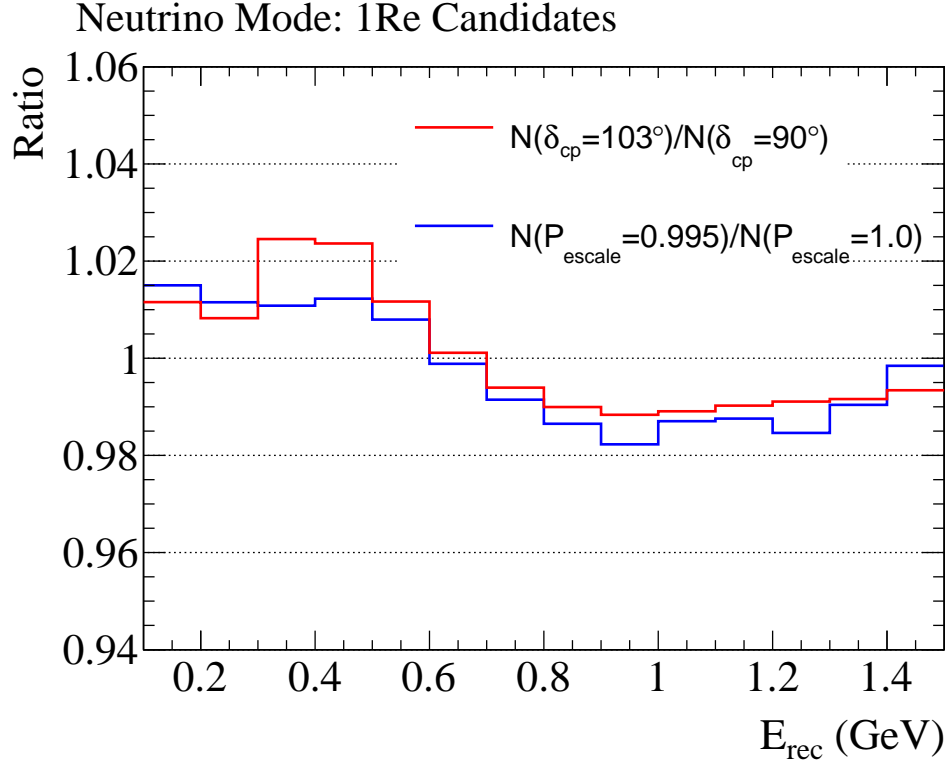
FIG. 16: The ratios to nominal predicted spectra ($\delta_{cp} = \pi/2$) for a δ_{cp} shift of $+13°$ and an energy scale shift of -0.5%. The ratios are shown for the 1R*e* samples in neutrino mode (top) and antineutrino mode (bottom). The ratios are calculated for the Hyper-K detector at 295 km and 2.5° off-axis.

CP-even term can be seen in the increased rate from 1.3 GeV and above for both neutrino and antineutrino mode. The CP-odd term causes an asymmetry in the normalization of the neutrino mode and antineutrino mode samples below 1 GeV. These effects can not be reproduced with a small variation of the energy scale parameter, as is the case for Hyper-K. This study shows that the constraint on δ_{cp} near $\delta_{cp} = \pi/2, 3\pi/2$ is sensitive to different systematic errors for Hyper-K and the Korean detector. It also shows that the fractional change to spectrum from the δ_{cp} variation is larger for the detector at a longer baseline, suggesting that the measurement is less likely to be systematics limited. The full impact of the Korean detector on the δ_{cp} precision will be shown in the following section where the physics sensitivities are presented.

D. Impact of the Korean detector on physics results

For the physics sensitivity studies presented here, it is assumed that two 187 kton tanks will be operated for 10 years×1.3 MW. For the initial studies, four configurations are considered:

- **JD×2** - Both tanks are located in Japan at the Tochibora site with a baseline of 295 km and an off-axis angle of 2.5°.

- **JD+KD at 2.5°** - One tank is located in Japan at a baseline of 295 km and an off-axis angle of 2.5°, while the second is located in Korea at a baseline of 1100 km and an off-axis angle of 2.5°.

- **JD+KD at 2.0°** - One tank is located in Japan at a baseline of 295 km and an off-axis angle of 2.5°, while the second is located in Korea at a baseline of 1100 km and an off-axis angle of 2.0°.

- **JD+KD at 1.5°** - One tank is located in Japan at a baseline of 295 km and an off-axis angle of 2.5°, while the second is located in Korea at a baseline of 1100 km and an off-axis angle of 1.5°.

Later in this section, the sensitivities for the Mt. Bisul site ($L = 1084$ km and OAA=1.3°) will also be presented.

Neutrino Mode: 1Re Candidates

N(δ_{cp}=103°)/N(δ_{cp}=90°)

N(P_{escale}=0.995)/N(P_{escale}=1.0)

Antineutrino Mode: 1Re Candidates

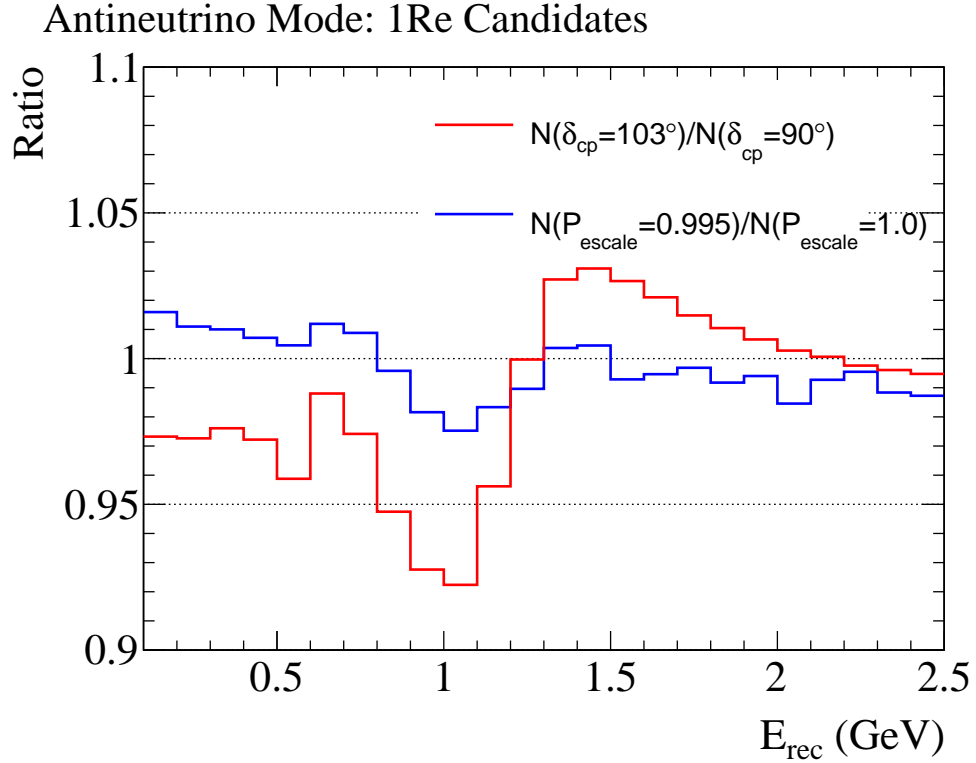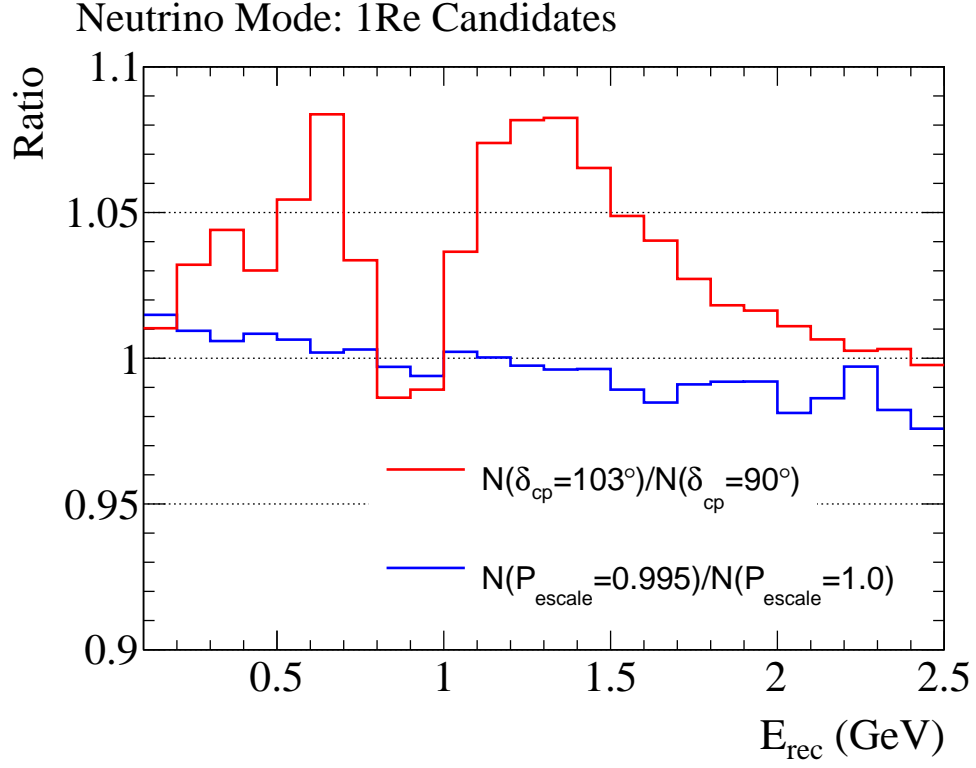N(δ_{cp}=103°)/N(δ_{cp}=90°)

N(P_{escale}=0.995)/N(P_{escale}=1.0)

FIG. 17: The ratios to nominal predicted spectra ($\delta_{cp} = \pi/2$) for a δ_{cp} shift of $+13°$ and an energy scale shift of -0.5%. The ratios are shown for the 1Re samples in neutrino mode (top) and antineutrino mode (bottom). The ratios are calculated for the Korean detector at 1100 km and $1.5°$ off-axis.

The initial physics sensitivity studies focus on 3 measurements: the determination of the mass ordering, the discovery of CP violation through the exclusion of the $\sin(\delta_{cp}) = 0$ hypothesis, and the precision measurement of δ_{cp}. In all cases, the sensitivities are evaluated on pseudo-data generated with the following true oscillation parameter values:

- $|\Delta m_{32}^2| = 2.5 \times 10^{-3}$ eV^2

- $\sin^2 \theta_{23} = 0.5$

- $\sin^2 \theta_{13} = 0.0219$

- $\Delta m_{21}^2 = 7.53 \times 10^{-5}$ eV^2

- $\sin^2 \theta_{12} = 0.304$

The pseudo-data are also generated for multiple values of δ_{cp} and both mass orderings, and the sensitivities are presented as a function of the true value of δ_{cp} and the mass ordering. In the fits to the pseudo-data, Δm_{32}^2, $\sin^2 \theta_{23}$ and δ_{cp} are free parameters with no prior constraints. $\sin^2 \theta_{13}$, $\sin^2 \theta_{12}$ and Δm_{21}^2 also vary in the fits, but they have prior Gaussian constraints with 1σ uncertainties of 0.0012, 0.041 and 0.18×10^{-5} eV^2 respectively. The prior uncertainties on these parameters are taken from the 2015 edition of the PDG Review of Particle Physics. The systematic parameters described in the previous section are also allowed to vary as nuisance parameters in the fit within their prior constraints. In all cases, the sensitivities are evaluated on the fit to the so-called Asimov set, i.e. the prediction for the nominal values of the oscillation parameter and systematic parameters. All four samples (neutrino mode 1Re, 1Rμ and antineutrino mode 1Re, 1Rμ) are used to construct a binned likelihood and the product of the pseudo-data likelihood is taken with the Gaussian priors for constrained oscillation parameters and systematic parameters to construct the full likelihood, L. To simplify the notation, we write $-2\log(L)$ as $\Delta\chi^2$.

The test statistic used for the mass ordering determination is:

$$T_{MH} = \sqrt{\Delta\chi_{WH}^2 - \Delta\chi_{CH}^2} \tag{3}$$

Here, $\Delta\chi_{WH}^2$ and $\Delta\chi_{CH}^2$ are the best-fit $-2\log(L)$ for the wrong and correct mass hierarchies respectively. In the Gaussian limit, the test parameter can be interpreted as the significance of the mass ordering determination. Here sensitivities are shown for the Hyper-K accelerator

neutrinos only and do not account for the additional constraint from Hyper-K atmospheric neutrinos.

The test statistic used for the CP violation discover potential is:

$$T_{CPV} = \sqrt{MIN[\Delta\chi^2_{BF}(\delta_{cp} = 0), \Delta\chi^2_{BF}(\delta_{cp} = \pi)] - \Delta\chi^2_{BF}} \tag{4}$$

Here, $\Delta\chi^2_{BF}(\delta_{cp} = 0)$ and $\Delta\chi^2_{BF}(\delta_{cp} = \pi)$ are the best-fit $-2\log(L)$ where δ_{cp} is fixed to one of the CP conserving values. The minimum of these two is used for the test statistic. $\Delta\chi^2_{BF}$ is the best-fit minimum of $-2\log(L)$ where δ_{cp} is allowed to vary. Two cases are treated for the CP violation studies. In the first case, the mass ordering is assumed to be known based on external measurements and the measurement using the Hyper-K atmospheric neutrinos. In the second case, the constraints from external measurements and Hyper-K atmospheric neutrinos are not used, in order to estimate the sensitivity from the accelerator neutrinos alone. When the mass ordering is determined with Hyper-K accelerator neutrinos alone, the sign of Δm^2_{32} is allowed to vary in the minimization procedure. The test parameter can be interpreted as the significance to exclude the CP conserving hypotheses.

For the evaluation of the δ_{cp} measurement precision the fitted value of δ_{cp} is scanned and the $-2\log(L)$ is minimized at each value of δ_{cp}, $i.e.$ the profiling method. The δ_{cp} values that correspond to a 1 unit change in $-2\log(L)$ relative to the minimum are taken as the bounds for the 68% confidence interval. The plotted 1σ error is the width of the 68% confidence interval divided by two.

The significances to reject the wrong mass ordering are shown in Fig. 18, and the fraction of δ_{cp} values for which a given significance is achieved is shown in Fig. 19. As is expected based on Fig. 13, the significance is largest for the configuration with the Korean detector at 1.5° off-axis since the more on-axis position gives more events in the 1-2 GeV range where the matter effect is large. For this configuration, the significance to reject the wrong mass ordering is greater than 6σ for most values of δ_{cp} and greater than 5σ for all values of δ_{cp}. The significance of the wrong mass ordering rejection degrades as the Korean detector is moved to more off-axis locations. However, even the configuration with 2.5° off-axis Korean detector has 3σ rejection sensitivity for most values of δ_{cp} and improved sensitivity over the configuration with both tanks in Japan for most values of δ_{cp}. Based on this study, it is clear that the sensitivity may be improved further by adding events above 1 GeV in reconstructed energy. This may be achieved by moving to a more on-axis position (see Mt. Bisul) or by

including multi-ring event reconstruction that allows the inclusion of higher energy events with one or more detected pions. The multi-ring event reconstruction will be the topic of a future study. Based on this study of the configurations with a detector in Korea, the accelerator neutrinos can provide an alternative measurement of the mass ordering that is complimentary to the measurement using atmospheric neutrinos. By combining the two measurements, an even stronger constraint can be obtained, and better sensitivity can be achieved earlier in the lifetime of the Hyper-K.

The plots showing the significance to reject the CP conserving hypotheses are in Fig. 20, and Fig. 21 shows the fraction of δ_{cp} values for which a given significance can be achieved. The fractions of true δ_{cp} values for which 3σ and 5σ sensitivity are achieved are listed in Table VI. When the mass ordering is already known, all four configurations have similar sensitivity, but the best sensitivity is available when the Korean detector is placed at $2.0°$ off-axis. It should be mentioned that in this study, it is assumed that the mass ordering is determined by external experiments and Hyper-K atmospheric neutrinos with a significance greater than the CP conservation rejection significance being studied. When the mass ordering is only determined by the accelerator neutrinos, the configuration with the Korean detector at $1.5°$ off-axis gives the largest fraction of true δ_{cp} values for which a 5σ discovery is possible. This is true because this configuration has the best sensitivity to determine the mass ordering, breaking the mass ordering-δ_{cp} degeneracy.

The evolution of the CP violation discovery potential with exposure is summarized in Fig. 22. At a 20 year×1.3 MW exposure, the presence of the Korean detector can increase the fraction of δ_{cp} values for which a 5σ discovery is possible by up to 8%. This is a 27% reduction in the number of δ_{cp} values for which a 5σ discovery of CP violation would not be possible.

The δ_{cp} measurement precision is shown in Fig. 23, and Fig. 24 shows the fraction of δ_{cp} values for which a given level of precision can be achieved. The configurations with the Korean detector give the best δ_{cp} precision on average. Near the CP conserving values, the configurations with the $2.0°$ and $1.5°$ off-axis Korean detectors have similar precision. However, near the maximally CP violating values of δ_{cp} the $1.5°$ off-axis configuration has $1.5°$ better precision for δ_{cp} than the $2.0°$ off-axis configuration. The configuration with the $1.5°$ off-axis Korean detector also improves on the precision of the configuration with 2 detectors in Japan by $3°$ near the maximally CP violating values of δ_{cp}. The precision
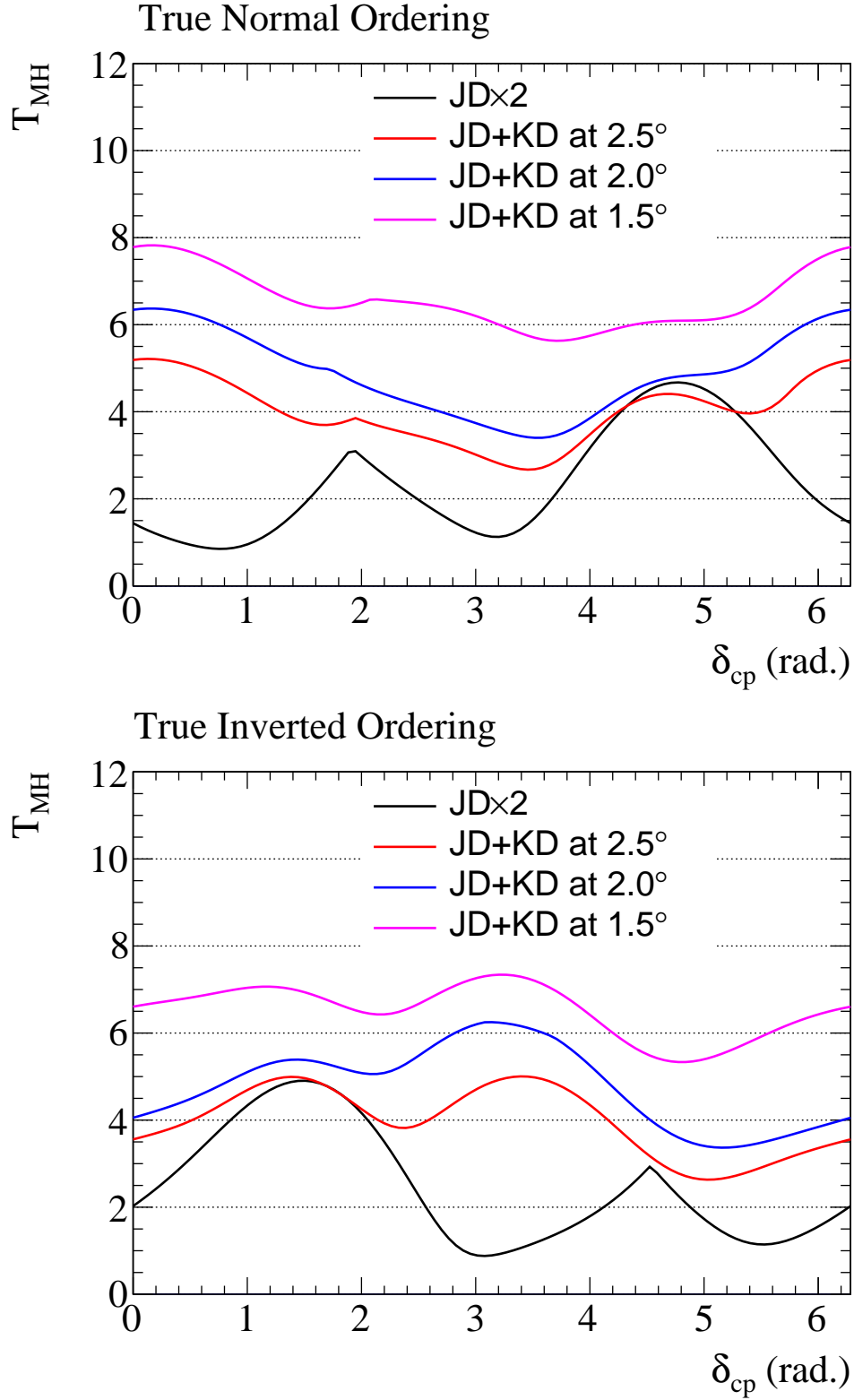
FIG. 18: The significance for the wrong mass ordering rejection as a function of the true value of δ_{cp} and the true mass ordering (top=normal, bottom=inverted).
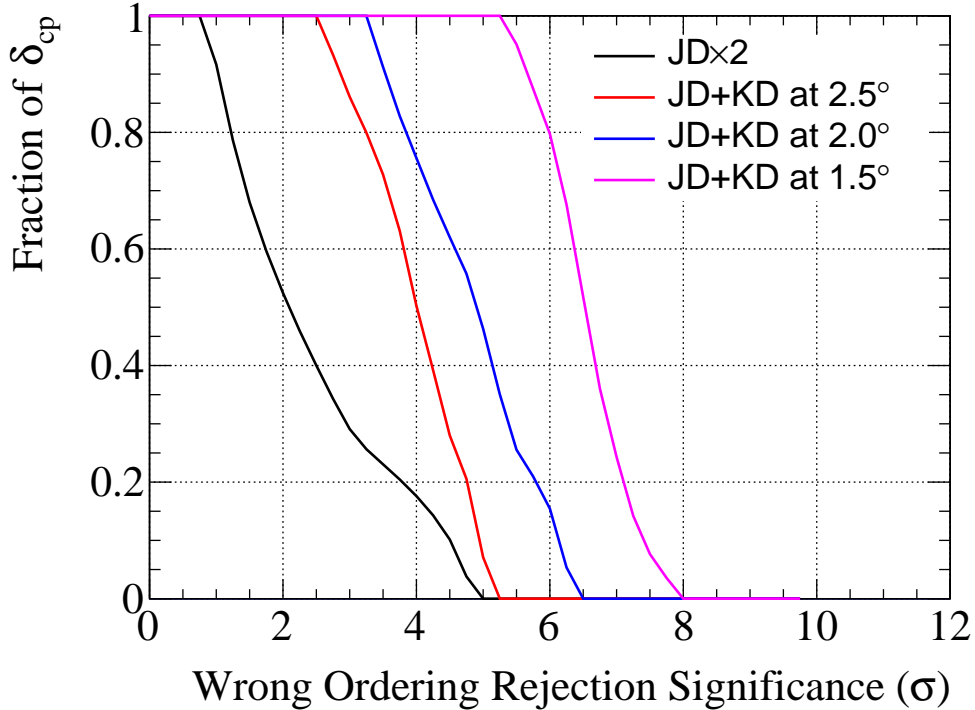
FIG. 19: The fraction of δ_{cp} values (averaging over the true mass ordering) for which the wrong hierarchy can be rejected with a given significance or greater.

TABLE VI: The fraction of true δ_{cp} values for which CP violation can be discovered at 3σ or 5σ.

	True NH, Known		True IH, Known		True NH, Unknown		True IH, Unknown	
	3σ	5σ	3σ	5σ	3σ	5σ	3σ	5σ
JD×2	0.74	0.55	0.74	0.55	0.52	0.27	0.50	0.28
JD+KD at 2.5°	0.76	0.58	0.76	0.59	0.76	0.48	0.72	0.30
JD+KD at 2.0°	0.78	0.61	0.78	0.61	0.77	0.55	0.79	0.51
JD+KD at 1.5°	0.77	0.59	0.77	0.59	0.77	0.59	0.77	0.59

for the configuration with 2 detectors in Japan is 3° better than what is presented in the Hyper-K design report. Further studies are necessary to determine if this difference arises due to differences in the systematic error model. However, it is likely that any additional systematic errors will more strongly impact the measurement with 2 detectors in Japan since
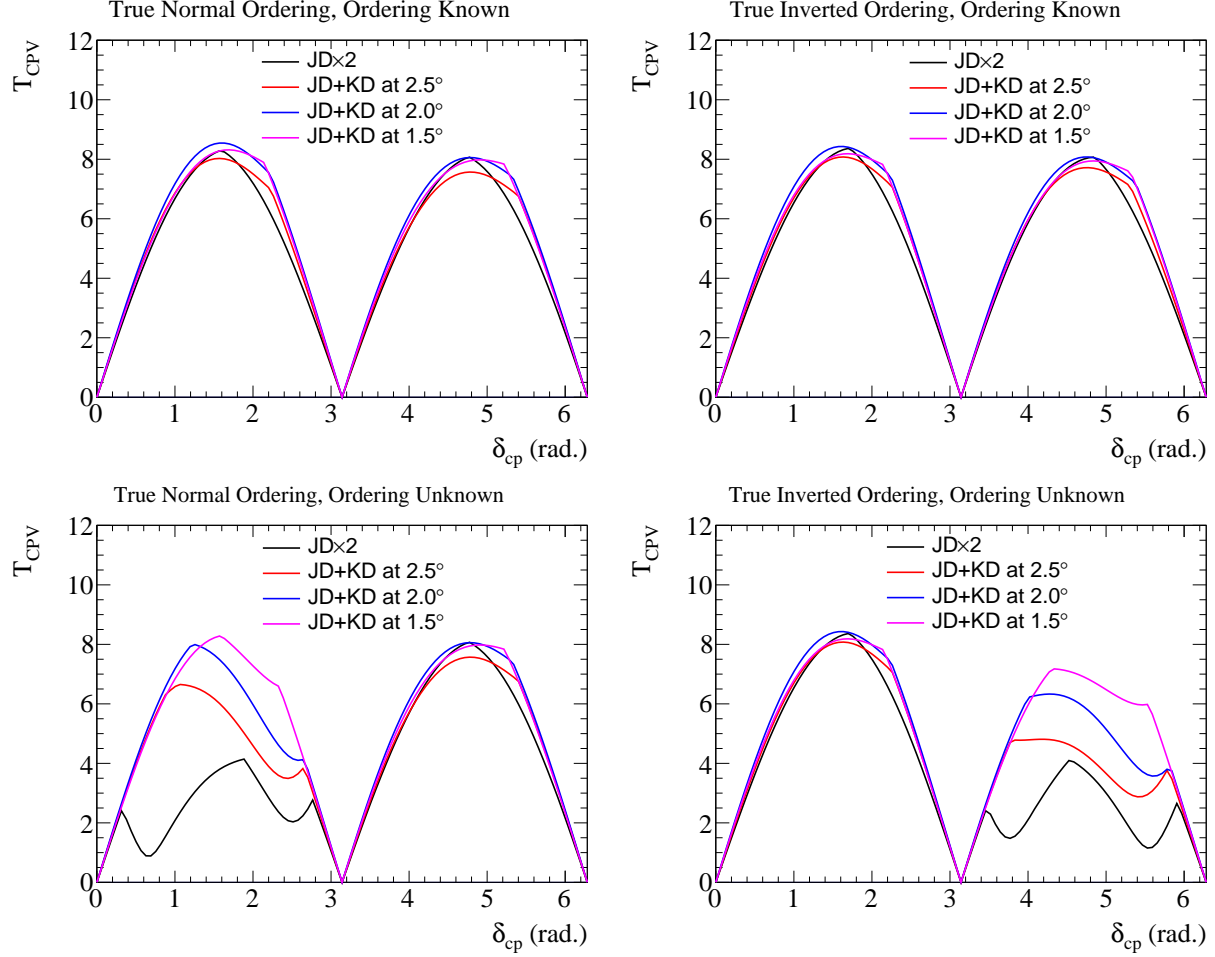
FIG. 20: The significance for CP conservation rejection as a function of the true value of δ_{cp} and the true mass ordering (left=normal, right=inverted). The top row shows the significance when the mass ordering is determined independently from the accelerator neutrinos, while the bottom row shows the significance when the mass ordering is determined only by accelerator neutrinos observed in the Hyper-K detectors.

the measurements at 295 km baseline are systematics limited, while the measurements at the 1100 km baseline are statistics limited.

The evolution of the δ_{cp} precision with exposure is summarized in Fig. 25. For the worst-case uncertainty, when δ_{cp} is near the maximally CP violation values, the relative advantage of the detector in Korea remains constant with exposure. It should be noted, however, that this may be an artifact of the systematic error model used in these studies, which likely underestimates the uncertainties on the shape of the observed spectra. For a more realistic
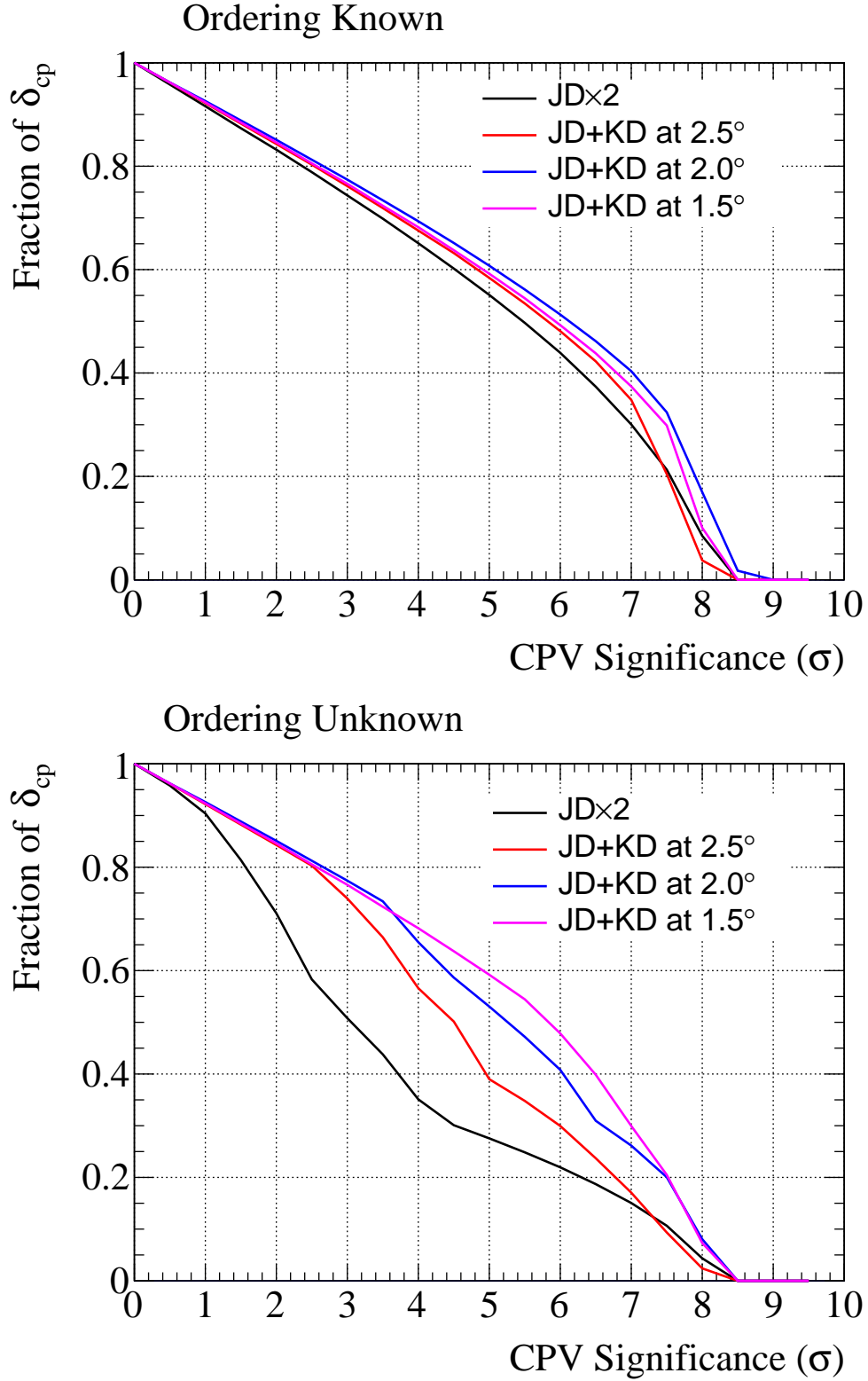
45

FIG. 21: The fraction of δ_{cp} values (averaging over the true mass ordering) for which the CP conserving values can be rejected with a given significance or greater. The top figure shows the significance when the mass ordering is determined independently from the accelerator neutrinos, while the bottom figure shows the significance when the mass ordering is determined only by accelerator neutrinos observed in the Hyper-K detectors.
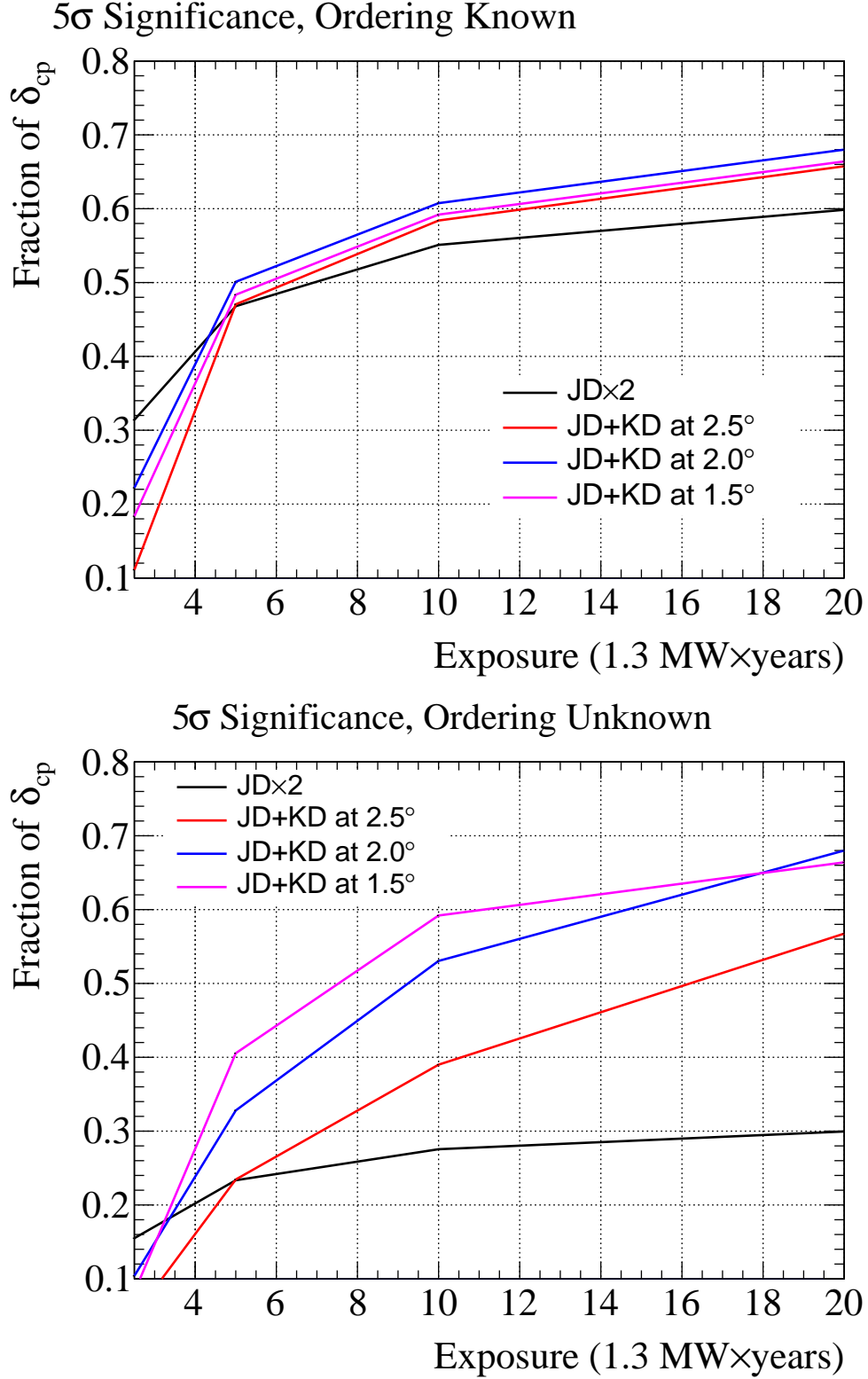
FIG. 22: The fraction of δ_{cp} values (averaging over the true mass ordering) with at least a 5σ significance to reject the CP conserving values of δ_{cp}. The top figure shows the significance when the mass ordering is determined independently from the accelerator neutrinos, while the bottom figure shows the significance when the mass ordering is determined only by accelerator neutrinos observed in the Hyper-K detectors.

systematic error model, the δ_{cp} resolution may be degraded, particularly for the detector in Japan which is more systematics limited.

1. Sensitivity studies for the Mt. Bisul site

The potential Mt. Bisul site is located at a baseline of 1088 km and an off-axis angle of 1.3°. The primary effect of the off-axis angle change from 1.5° to 1.3° is to decrease the (anti)neutrino flux at 700 MeV by $\sim 10\%$ while increasing flux above 1.2 GeV by $\sim 50\%$. With these flux changes, it is expected that the Mt. Bisul location should provide better sensitivity to determine the mass ordering, while the CP violation discovery potential may be slightly degraded. The wrong mass ordering rejection significances including the Mt. Bisul configuration are shown in Fig. 26. The wrong mass ordering rejection significance is largest for the Mt. Bisul configuration for all true values of the mass ordering and δ_{cp}, and is above 7σ for almost all values.

The CP conservation rejection significances including the Mt. Bisul configuration are shown in Fig. 27. There is little change to the fraction of δ_{cp} values with 3σ or 5σ rejection compared to the configuration with the Korean detector at 1.5° off-axis. For all cases of the true mass ordering and prior knowledge of the mass ordering, the fraction of δ_{cp} values with 3σ or 5σ significance is reduced by less than 0.01 compared to the 1.5° off-axis configuration. For the scenarios where the mass ordering is determined by the accelerator neutrinos only, better CP conservation rejection is achieved for some values of δ_{cp} where the improved wrong mass ordering rejection impacts the CP violation measurement.

The δ_{cp} precision is shown in Fig. 28. Near the maximally CP violation values, there is a slight improvement of the precision, indicating that the measurement is in part due to the spectrum distortion in the > 1 GeV region arising from the $\cos(\delta_{cp})$ dependent term. Near the CP conserving values, there is a very small degradation of the precision, but the Mt. Bisul configuration still provides better precision than the configuration with the 2.5° off-axis Korean detector.
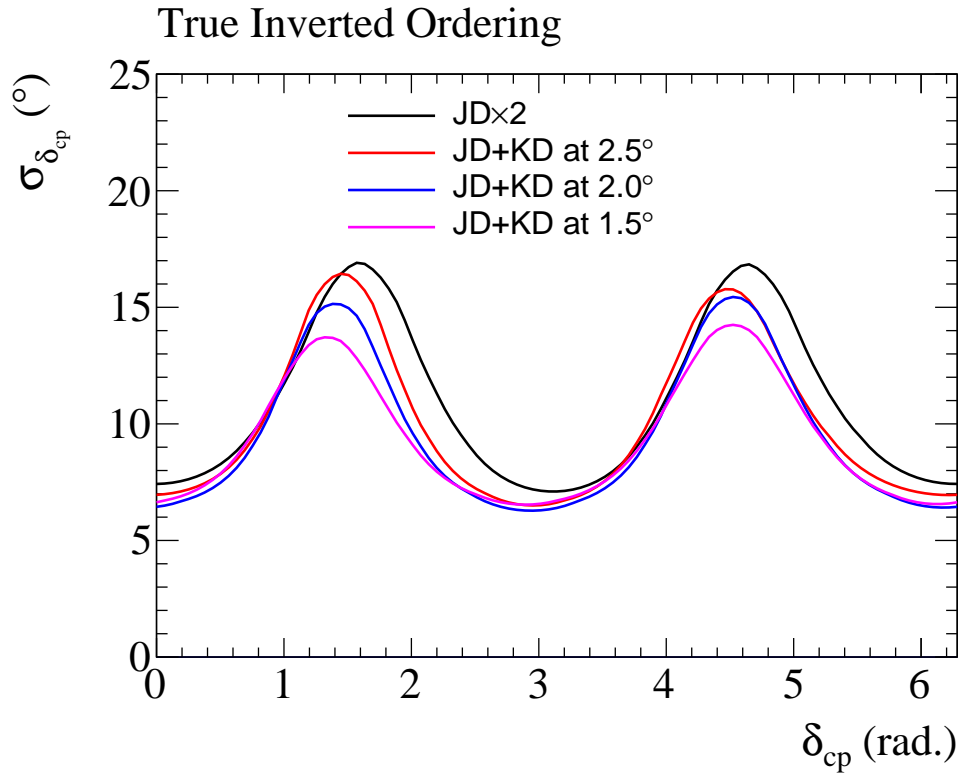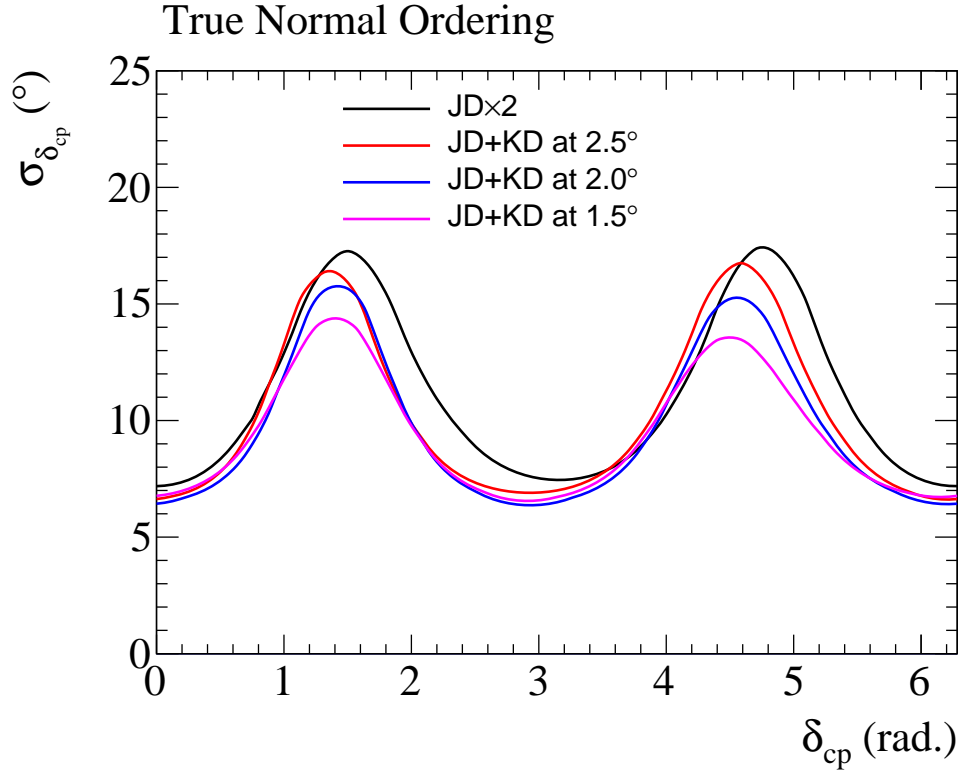
FIG. 23: The 1σ precision of the δ_{cp} measurement as a function of the true δ_{cp} value. Here, it is assumed there is no prior knowledge of the mass ordering.
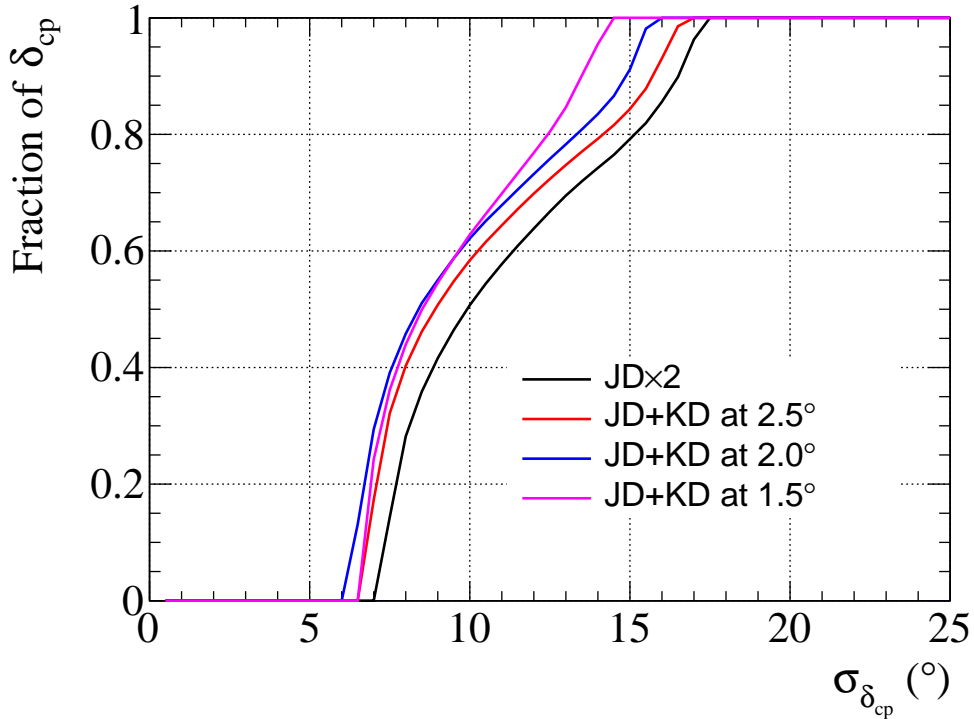
FIG. 24: The fraction of δ_{cp} values (averaging over the true mass ordering) for which a given precision or better on δ_{cp} can be achieved.

IV.   ADDITIONAL BENEFITS

In addition to the long baseline program with multiple baselines, there are potential benefits in the non-accelerator program by placing the second detector in Korea, especially with its prospective deeper site. There are two main benefits that arise from the second Hyper-K detector in Korea. The first benefit is from the deeper detector site which will result in a reduction of muon flux and isotope production from spallation. A second advantage comes from the geographical separation between two detectors.

In the following, we discuss possible enhancement of science capabilities that a second detector at a deep site in Korea brings compared to two Hyper-K detectors in close proximity in Japan. Although detailed geological information is not yet available, all the candidate sites currently considered are under mountains with $> 1,000$ m height. Considering tunnel entrance positions actual overburdens are expected to be greater than 820 m ($\sim$2,200 meters-water-equivalent, m.w.e.). With this overburden, the isotope production from muon spalla-
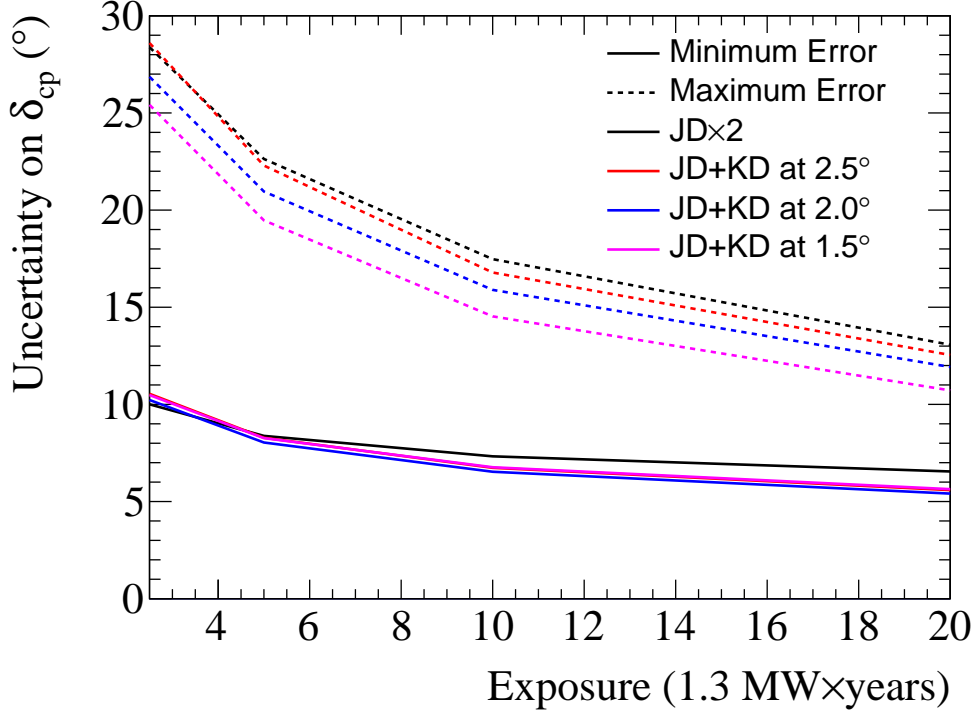
FIG. 25: The evolution of the δ_{cp} measurement precision with exposure. The "Minimum" and "Maximum" errors are the uncertainties at the true δ_{cp} and mass ordering values with the best and worst measurement resolution respectively.

tion is expected to be smaller than the first tank in Japan (with an overburden of 650 meters of rock or 1,750 m.w.e.) [42]. In future, more realistic estimate with geological information around the candidate site is necessary to evaluate the expected background level.

A. Solar, supernova, and reactor neutrinos

A lower spallation background level would result in better sensitivity for solar neutrino measurements. The day/night asymmetry due to the MSW matter effect [29–31] in the Earth is expected to be larger in the higher energy region of the ^{8}B neutrino spectrum, where the spallation is dominant background source. The hep solar neutrinos, which have the highest energy among solar neutrinos, could provide new information on solar physics, because the production regions of the ^{8}B and hep neutrinos are different in the Sun. Lower
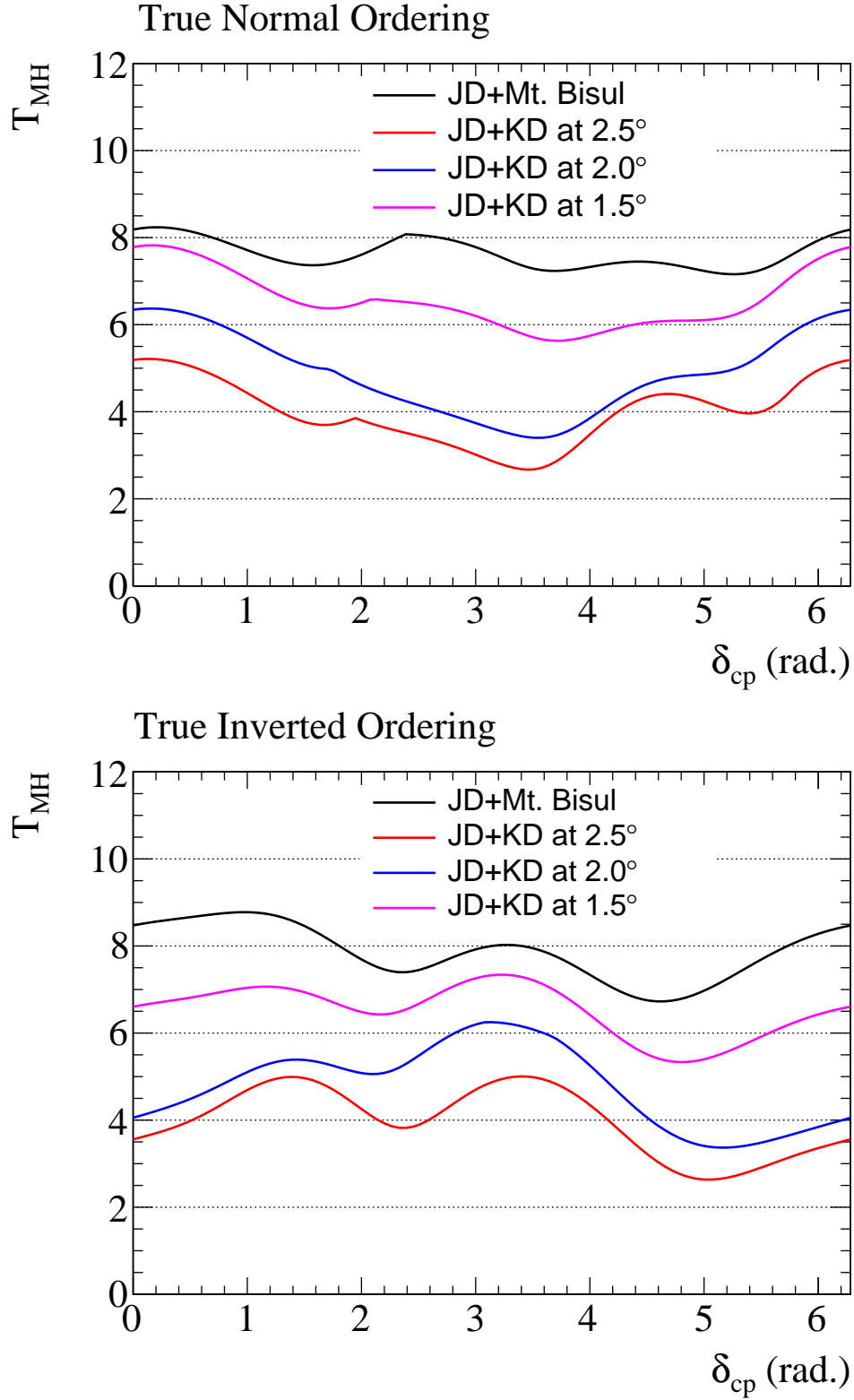
FIG. 26: The significance for the wrong mass ordering rejection as a function of the true value of δ_{cp} and the true mass ordering (top=normal, bottom=inverted). Results are shown for the Mt. Bisul site and the generic Korean sites.
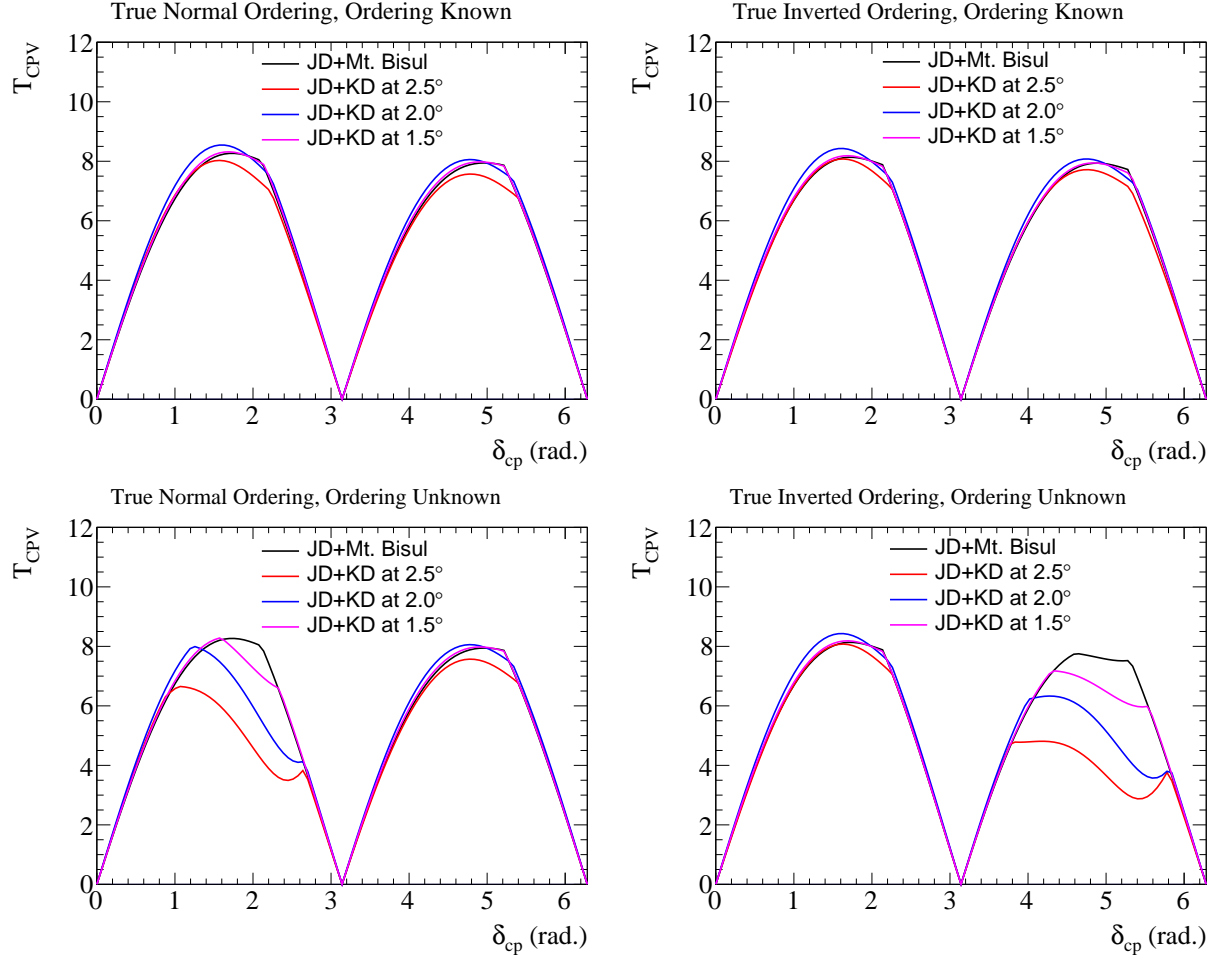
FIG. 27: The significance for CP conservation rejection as a function of the true value of δ_{cp} and the true mass ordering (left=normal, right=inverted). The top row shows the significance when the mass ordering is determined using external data and Hyper-K atmospheric neutrinos, while the bottom row shows the significance when the mass ordering is determined only by accelerator neutrinos observed in the Hyper-K detectors . Results are shown for the Mt. Bisul site and the generic Korean sites.

spallation rate would enhance the sensitivity to hep solar neutrinos. With lower background, short time variability of the temperature in the solar core could be monitored with better sensitivity or shorter time scale. The sensitivity to the energy spectrum upturn might be improved thanks to the lower background level in the higher energy region, which gives the baseline for the spectrum shape.

The neutrinos produced by all of the supernova explosions since the beginning of the
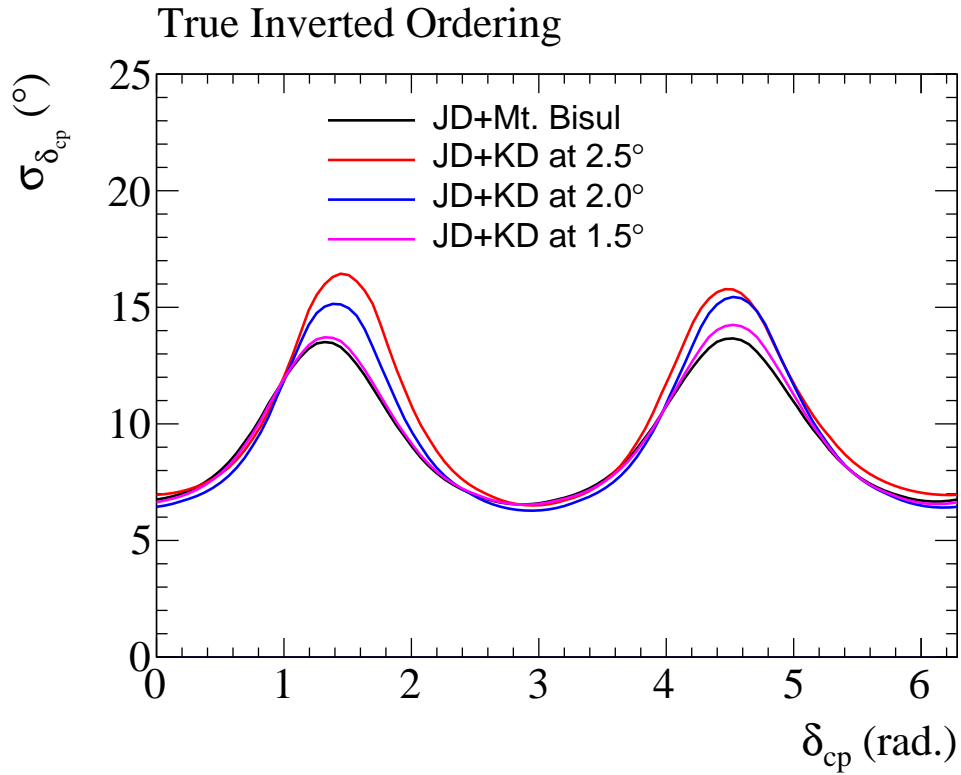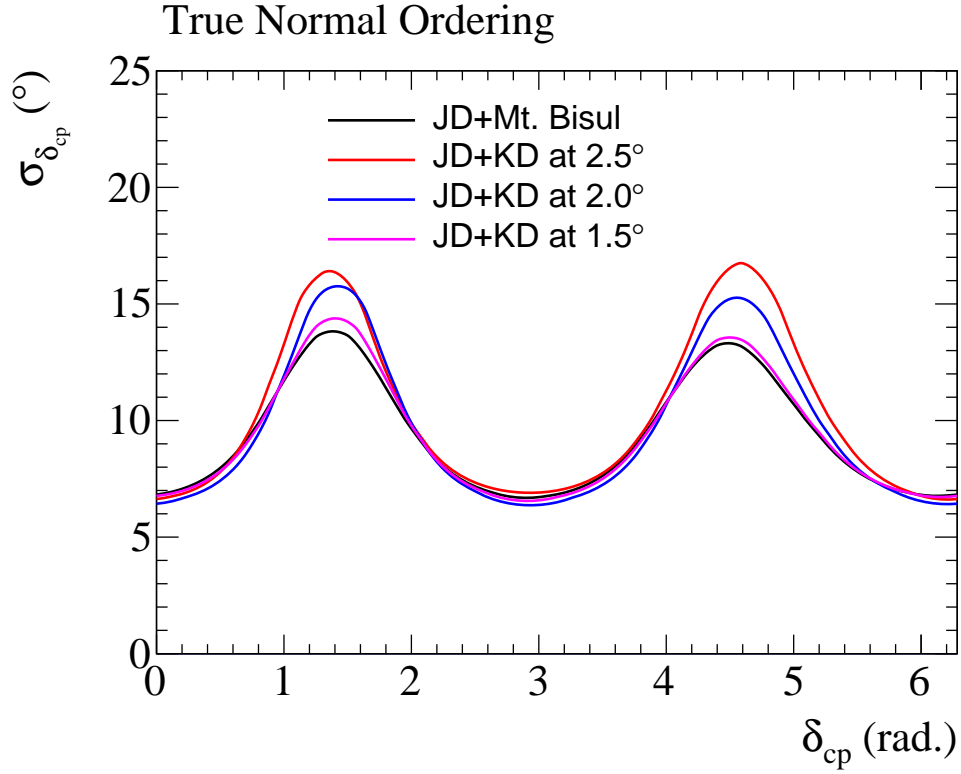
FIG. 28: The 1σ precision of the δ_{cp} measurement as a function of the true δ_{cp} value. Results are shown for the Mt. Bisul site and the generic Korean sites.

universe are called supernova relic neutrinos (SRN). A lower spallation background rate will enhance the SRN detection capability below 20 MeV, which is important for the measurement of SRN energy spectrum and thus study of the history of supernova bursts. With a capability to tag neutrons, it will be also possible to detect neutrinos from nuclear reactors in Korea using inverse beta decay.

B. Neutrino geophysics

The inner Earth chemical composition is one of the most important properties of our home planet. While Earth's matter density is well known through seismic measurements [41], the inner chemical composition is much less understood [32]. Neutrino oscillations depend on the electron density of the medium that is traversed by the neutrinos [29, 30], hence, the electron density distribution of the Earth can be reconstructed from the neutrino energy spectrum, and the chemical composition distribution of the Earth can be constrained for a given mass density distribution [33, 34]. Hyper-K is expected to be the first experiment that could experimentally confirm an iron Earth core with respect to lead or water at a $3\ \sigma$ level [19]. The measurement relies on precisely measuring atmospheric muon neutrino disappearance and electron neutrino appearance in the energy range of $1 - 8$ GeV as function of the zenith angle. A Korean detector will bring the benefit of having two detectors at different locations, which could potentially lead to reduced systematic uncertainties related to the atmospheric neutrino flux. In the case of a nearby supernova, the different detector locations might also provide sensitivity to the Earth composition due to the different path of the burst neutrinos through the Earth. For a single detector it might not be possible to uniquely disentangle matter effects from supernova burst neutrino properties.

C. Dark matter searches

Hyper-K can search for physics beyond the standard model in the form of self-annihilating dark matter captured in the Sun, Earth or from the Galactic dark matter halo. Super-K has demonstrated this physics potential through the world's best constraints on spin-dependent scattering of dark matter with matter [35]. Hyper-K can improve upon Super-K's results and is expected to provide the best indirect dark matter search sensitivities for masses

below 100 GeV. As the background to a neutrino signal from dark matter annihilation in the Sun comes from atmospheric neutrinos a benefit from a second site could come from reduced systematic uncertainties associated with atmospheric neutrino fluxes. A neutrino signal originating from the decays of the dark matter annihilation products in the Sun is also accompanied by a high multiplicity stopped meson decay low-energy neutrino signal from hadronic showers of the annihilation products in the center of the Sun [36–38]. The expected signal consists of neutrinos of a few ten's of MeV from muon decays at rest in the Sun as well as neutrino line signals at 29.8 MeV and 235.5 MeV from two-body charged pion and kaon decays at rest. The possible addition of gadolinium in water [39] would reduce (invisible muon) backgrounds significantly for this signal, which can very efficiently be detected through the inverse beta decay reaction [36].

D. Non standard neutrino interactions

T2HKK with the $\nu_\mu(\bar{\nu}_\mu)$ disappearance experiments could be also a powerful probe of nonstandard physics related with neutrinos. In Ref. [40], various types of non-standard new physics scenarios for neutrinos have been considered: (i) quantum decoherence, (ii) tiny violation of Lorentz symmetry with/without CPT invariance, and (iii) nonstandard neutrino interactions with matter. In most cases, the T2HKK setup can make significant improvements on the bounds on possible new physics effects on neutrino sectors, since two detector system can measure spectral distortion of neutrino beams more accurately than one detector systems. See Tables I, II and Fig. 6 in Ref. [40] for more details.

V. SUMMARY AND CONCLUSION

Sensitivity studies have been performed comparing several configurations of T2HKK, where one detector module is placed at Kamioka 2.5° off-axis and 295 km from the J-PARC neutrino beam and the other is placed in Korea $1° - 3°$ off-axis with a baseline of $1100-1300$ km. Most of the systematic error estimates used in this study are based on the current systematic uncertainties used in recent T2K oscillation analyses [27]. There are several candidate sites for the detector in Korea. Two candidate sites are particularly attractive for the detector. The site of Mt. Bisul (Mt. Bohyun) with 1084 (1126) m in

height is situated at $1.3°(2.2°)$ off-axis and 1088 (1040) km baseline distance. These studies illustrate that a larger matter effect and the second oscillation maximum occurrence with a detector in Korea can improve sensitivity for determining the neutrino mass ordering and leptonic δ_{CP} measurements, with respect to the 2nd Hyper-K detector in Kamioka. For example, the significance of rejecting a wrong mass ordering is greater than 6 σ for all values of δ_{CP} at the Mt. Bisul site. They also illustrate an enhancement coming from the T2HKK configuration if one combines information from two significantly different baselines. Searches for non-standard neutrino interactions are also expected to be improved.

The large overburden (> 800 m) of the candidate sites in Korea provides additional benefits for low energy neutrino physics including the study of solar neutrinos and the search for supernova neutrinos due to a lower spallation background rate.

Further sensitivity studies with more realistic and smaller systematic uncertainties will be performed in the near future. They will provide more improved sensitivities for neutrino mass ordering and the CP violation phase measurement. Additional benefits for low energy neutrino physics will be estimated in a more quantitative way. Based on the potential for significant improvements in physics sensitivities, T2HKK shows a viable and attractive option as an alternative to the default T2HK configuration with two detector modules in Kamioka.

ACKNOWLEDGEMENTS

[1] K. Abe *et al.* (Hyper-Kamiokande Working Group), arXiv:1412.4673 (2015); K. Abe *et al.* [Hyper-Kamiokande Proto-Collaboration], PTEP **2015**, 053C02 (2015) [arXiv:1502.05199 [hep-ex]].

[2] Y. Fukuda *et al.* (Super-Kamiokande Collaboration), Phys. Rev. Lett. **81**, 1562 (1998).

[3] S. B. Kim, in Proceedings of the KOSEF-JSPS Joint Seminar on New Developments in Neutrino Physics, Seoul, Korea, 2000 (Korea Institute for Advanced Study, Seoul, 2000), p. 182.

[4] K. Hagiwara, Nucl. Phys. Proc. Suppl. **137**, 84 (2004) [hep-ph/0410229].

[5] M. Ishitsuka, T. Kajita, H. Minakata and H. Nunokawa, Phys. Rev. D **72**, 033003 (2005).

[6] T. Kajita, H. Minakata, S. Nakayama, and H. Nunokawa, Phys. Rev. D **75**, 013006 (2007).

[7] F. Dufour, T. Kajita, E. Kearns and K. Okumura, Phys. Rev. D **81**, 093001 (2010).

[8] K. Hagiwara, N. Okamura, K. Senda, Phys. Lett. B **637**, 266 (2006), Erratum: Phys. Lett. B **641**, 491 (2006).

[9] K. Hagiwara, N. Okamura, K. Senda, Phys. Rev. D **76**, 093002 (2007).

[10] T. Kajita and H. Minakata, "Highlights in the T2KK Workshops in 2005 and 2006", `http://www-rccn.icrr.u-tokyo.ac.jp/workshop/T2KK07/proceedings/t2kk-pdf/003-014.pdf`; T. Kajita, S.B. Kim, A. Rubbia, arXiv: 0808.0650 (2008); 3rd International Workshop on a Far Detector in Korea for the J-PARC Neutrino Beam 30 Sep - 1 Oct 2007. Tokyo, Japan PROCEEDINGS. Edited by T. Kajita, S.B. Kim. Tokyo, Univ. Acad. Pr., 2008. 173p.

[11] K. Abe *et al.* [T2K Collaboration], Phys. Rev. Lett. **107**, 041801 (2011) [arXiv:1106.2822 [hep-ex]].

[12] Y. Abe *et al.* (Double Chooz Collaboration), Phys. Rev. Lett. **108**, 131801 (2012).

[13] F. P. An *et al.* (Daya Bay Collaboration), Phys. Rev. Lett. **108**, 171803 (2012).

[14] J. K. Ahn *et al.* (RENO Collaboration), Phys. Rev. Lett. **108**, 191802 (2012).

[15] K. Abe *et al.* [T2K Collaboration], Phys. Rev. Lett. **112**, 061802 (2014). [arXiv:1311.4750 [hep-ex]]

[16] Y. Abe *et al.* (Double Chooz Collaboration), JHEP **1410**, 86 (2014).

[17] F. P. An *et al.* (Daya Bay Collaboration), Phys. Rev. Lett. **115**, 111802 (2015).

[18] J. Choi *et al.* (RENO Collaboration), Phys. Rev. Lett. **116**, 211802 (2016).

[19] K. Abe *et al.* [Hyper-Kamiokande Proto-Collaboration], "Hyper-Kamiokande Design Report"

KEK-PREPRINT-2016-21, ICRR-REPORT-701-2016-1.

[20] K. Abe *et al.* [T2K Collaboration], Nucl. Instrum. Meth. A **659**, 106 (2011) [arXiv:1106.1238 [physics.ins-det]].

[21] S. Bhadra *et al.* [nuPRISM Collaboration], arXiv:1412.3086 [physics.ins-det]; C. Andreopoulos *et al.*, arXiv:1606.08114 [physics.ins-det].

[22] I. Girardia, S. T. Petcov, and A. V. Titov Nucl. Phys. B **894**, 733 (2015).

[23] H. Nunokawa, S. J. Parke and J. W. F. Valle, Prog. Part. Nucl. Phys. **60**, 338 (2008) [arXiv:0710.0554 [hep-ph]].

[24] Y. Hayato, Acta Phys. Polon. B **40**, 2477 (2009).

[25] http://www.phy.duke.edu/~raw22/public/Prob3++/

[26] K. Hagiwara, N. Okamura and K.I. Senda, JHEP **1109**, 082 (2011) [arXiv:1107.5857 [hep-ph]].

[27] K. Abe *et al.* [T2K Collaboration], Phys. Rev. D **91**, 072010 (2015) [arXiv:1502.01550 [hep-ex]].

[28] M. Day and K. S. McFarland, Phys. Rev. D **86**, 053003 (2012) [arXiv:1206.6745 [hep-ph]].

[29] L. Wolfenstein, Phys. Rev. D **17**, 2369 (1978).

[30] S. P. Mikheev and A. Y. Smirnov, Sov. J. Nucl. Phys. **42**, 913 (1985); Yad. Fiz. **42**, 1441 (1985).

[31] S. P. Mikheev and A. Y. Smirnov, Nuovo Cim. C **9**, 17 (1986).

[32] W. McDonough and S. Sun, Chem. Geol. **120**, 223 (1995).

[33] C. Rott, A. Taketa and D. Bose, Scientific Reports 5, Article number: 15225 (2015) [arXiv:1502.04930 [physics.geo-ph]].

[34] W. Winter, Nucl. Phys. B **908**, 250 (2016) [arXiv:1511.05154 [hep-ph]].

[35] K. Choi *et al.* [Super-Kamiokande Collaboration], Phys. Rev. Lett. **114**, 141301 (2015) [arXiv:1503.04858 [hep-ex]].

[36] C. Rott, J. Siegal-Gaskins and J. F. Beacom, Phys. Rev. D **88**, 055005 (2013) [arXiv:1208.0827 [astro-ph.HE]].

[37] N. Bernal, J. Martin-Albo and S. Palomares-Ruiz, JCAP **1308**, 011 (2013) [arXiv:1208.0834 [hep-ph]].

[38] C. Rott, S. In, J. Kumar and D. Yaylali, JCAP **1511**, 039 (2015) [arXiv:1510.00170 [hep-ph]].

[39] J. F. Beacom and M. R. Vagins, Phys. Rev. Lett. **93**, 171101 (2004) [hep-ph/0309300].

[40] N. C. Ribeiro, H. Nunokawa, T. Kajita, S. Nakayama, P. Ko and H. Minakata, Phys. Rev. D

77, 073007 (2008) [arXiv:0712.4314 [hep-ph]].

[41] A. M. Dziewonski and D. L. Anderson, Phys. Earth Planet. Interiors **25**, 297 (1981).

[42] As a reference, for the Super-K site (1,000 m overburden), the muon spallation background rate is a factor of four smaller than what is expected for the HK first tank site.